J. Amer. Soc. Hort. Sci. 144(4):219–235. 2019. https://doi.org/10.21273/JASHS04629-18

Transcriptome Analysis of *Chrysanthemum lavandulifolium* Response to Salt Stress and Overexpression a K^+ Transport *ClAKT* Gene-enhanced Salt Tolerance in Transgenic *Arabidopsis*

He Huang[1], Yuting Liu[1], Ya Pu, Mi Zhang, and Silan Dai[2]

Beijing Key Laboratory of Ornamental Plants Germplasm Innovation and Molecular Breeding, National Engineering Research Center for Floriculture, Beijing Laboratory of Urban and Rural Ecological Environment and College of Landscape Architecture, Beijing Forestry University, Beijing, 100083, China

Additional index words. halophyte, Illumina sequencing, physiological analyses, potassium transporter, salinity

Abstract. **Plant growth and development are significantly affected by salt stress. *Chrysanthemum lavandulifolium* is a halophyte species and one of the ancestors of chrysanthemum (*C.* ×*morifolium*). Understanding how this species tolerates salt stress could provide vital insight for clarifying the salt response systems of higher plants, and chrysanthemum-breeding programs could be improved. In this study, salt tolerance was compared among *C. lavandulifolium* and three chrysanthemum cultivars by physiological experiments, among which *C. lavandulifolium* and Jinba displayed better tolerance to salt stress than the other two cultivars, whereas Xueshan was a salt-sensitive cultivar. Using the transcriptome database of *C. lavandulifolium* as a reference, we used digital gene expression technology to analyze the global gene expression changes in *C. lavandulifolium* seedlings treated with 200 mM NaCl for 12 hours compared with seedlings cultured in normal conditions. In total, 2254 differentially expressed genes (DEGs), including 1418 up-regulated and 836 down-regulated genes, were identified. These DEGs were significantly enriched in 35 gene ontology terms and 29 Kyoto Encyclopedia of Genes and Genomes pathways. Genes related to signal transduction, ion transport, proline biosynthesis, reactive oxygen species scavenging systems, and flavonoid biosynthesis pathways were relevant to the salt tolerance of *C. lavandulifolium*. Furthermore, comparative gene expression analysis was conducted using reverse transcription polymerase chain reaction to compare the transcriptional levels of significantly up-regulated DEGs in *C. lavandulifolium* and the salt-sensitive cultivar Xueshan, and species-specific differences were observed. The analysis of one of the DEGs, *ClAKT*, an important K^+ transport gene, was found to enable transgenic *Arabidopsis thaliana* to absorb K^+ and efflux Na^+ under salt stress and to absorb K^+ under drought stress. The present study investigated potential genes and pathways involved in salt tolerance in *C. lavandulifolium* and provided a hereditary resource for the confinement of genes and pathways responsible for salt tolerance in this species. This study provided a valuable source of reference genes for chrysanthemum cultivar transgenesis breeding.**

About 20% of inundated rural land worldwide is adversely influenced by salt content, which influences the profitability and quality of crops (Flowers and Colmer, 2015). Large amounts of salt cause hyperosmotic stress and particle cytotoxicity in higher plants and require supplements for farmlands (Deinlein et al., 2014; Katiyar-Agarwal et al., 2005). It is extremely difficult to enhance tolerance to salt stress in plants by genetic engineering because the reaction to salt stress in plants is relatively controlled by cascades of molecular networks, and such a significant number of pathways and genes is associated with the process of salt tolerance that it is a profoundly complex process (Deinlein et al., 2014). In higher plants, the salt stress signal is first recognized at the membrane level by receptors, which produce secondary signal molecules, such as Ca^{2+}, inositol phosphates, responsive oxygen species (ROS), and abscisic acid (ABA) (Baxter et al., 2014; Chen et al., 2017; Huang et al., 2012; Yoshida et al., 2014). The stress signal is then transduced into the cell nucleus and actuates various stress responsive pathways that eventually prompt plant adjustment to salt stress. Proposed mechanisms of salt response in plants depend on a few perspectives, such as ion compartmentalization, homeostasis, prohibition and discharge, and transport (Deinlein et al., 2014; Hasegawa, 2013; Wang et al., 2018a). Producing and accumulating compatible solutes and osmolytes also was reported to be imperative for managing the high concentration of salt in higher plants (Flowers and Colmer, 2015). Moreover, many reports have shown that salt tolerance in plants can be mostly clarified by the scavenging properties of antioxidative proteins (Bose et al., 2013; Rady et al., 2018). Plants that can survive and reproduce in sodium chloride (NaCl) concentrations 200 mM or greater are called halophytes (Flowers and Colmer, 2008). Halophytes have evolved many growth responses to increase salt tolerance, of which the most important strategy is controlled uptake and compartmentalization of Na^+, K^+, and Cl^- and the synthesis of compatible organic solutes (Rozema and Schat, 2013).

Received for publication 27 Dec. 2018. Accepted for publication 29 Apr. 2019. This work was supported by the Fundamental Research Funds for the Central Universities (No. 2015ZCQ-YL-03) and National Natural Science Foundation of China (Grant no. 31501793).

[1]These authors contributed equally.

[2]Corresponding author. E-mail: silandai@sina.com.

Although we have accumulated a great deal of common knowledge about salt tolerance mechanisms in plants, complete understanding of the specific response mechanisms for salt tolerance in higher plants, especially in halophytes, is still lacking. *Chrysanthemum* ×*morifolium* is one of the most important ornamental crops in the world. In China, the chrysanthemum industry, especially the cut flower and potted chrysanthemum industry, is now flourishing, and *C.* ×*morifolium* is becoming one of the most important commercially used floral crops. However, planting areas for *C.* ×*morifolium* are limited due to its sensitivity to abiotic stress, especially drought and salt stress. Due to the large and complex genome and complicated allohexaploid genetic background ($2n = 6x = 54$), very few gene resources are currently available for transgenic breeding of *C.* ×*morifolium* to protect against abiotic stress. Wild ancestors are major genetic resources for cultivating plant tolerance to both abiotic and biotic stresses. *C. lavandulifolium* is a major origin diploid species ($2n = 2x = 18$) of cultivated *C.* ×*morifolium* and has a relatively small genome (C-value = 2.46 Gbp). This species is widely distributed in slopes, rocks, valleys, banks, unclaimed lands, and loess hilly lands in north China, suggesting that it is a drought- and salt-tolerance species (Ling and Shi, 1983). This species can survived in 300 mM NaCl treatment and belongs to halophyte plants (Huang et al., 2012a). Previous work have identified some salt-induced genes in *C. lavandulifolium*, such as *AKT*, *NAC* (Huang et al., 2012a, 2012b), and *CBF* (Gao et al., 2018) gene family members. However, as genetically complex responses to salt stresses are multigenic traits, isolation of a few genes cannot explain the salt response mechanism.

Next-generation sequencing technology is a quick strategy to investigate a variety of stress reactions on a global transcriptional scale in non-model plant species for which whole-genome sequencing has not been completed. In addition, these systems have been used successfully to examine the molecular mechanisms of responses to abiotic stresses in numerous non-model plant species and halophytes. For example, genes encoding ion transporters and ROS scavenging system proteins in *Reaumuria trigyna* (Dang et al., 2013) and genes related to ion transport, energy metabolism, and hormone-reaction pathways in *Halogeton glomeratus* (Wang et al., 2015) were the most significant upregulated pathways under salt stress. In this study, digital gene expression (DGE) was used to analyze the transcriptomic changes in *C. lavandulifolium* leaves treated with salt (200 mM NaCl) for 12 h compared with the seedlings cultured in typical conditions to isolate genes and Encyclopedia of Genes and Genomes (KEGG) pathways with significant transcriptional changes. Comparative gene expression analysis was carried out by reverse transcription polymerase chain reaction (RT-PCR) to compare the transcriptional levels of critically upregulated DEGs in *C. lavandulifolium* and *C.* ×*morifolium* 'Xueshan' to explore species-specific mechanisms and genes related to these genotypes. Data generated in this study provide a valuable resource for future work on the salt response component of *C. lavandulifolium* and directed transgenic breeding of chrysanthemum cultivars.

Materials and Methods

Plant materials and stress treatments. Plant materials used for physiological analyses and quantitative (q)RT-PCR analysis were cloned propagules of *C. lavandulifolium* and three chrysanthemum cultivars. The *C. lavandulifolium* clones used in the present study are extremely salt-tolerant by our previous study (Huang et al., 2012a). For the three chrysanthemum cultivars, Xueshan and Xueshen were bred by our group, and Jinba was the main chrysanthemum cultivar. Stem cuttings with a single node of the aforementioned cultivars were used as explants, and these stem cuttings were cultured on Murashige and Skoog (MS) medium. After 7 d (when roots reached 2–3 cm), sterile plantlets were transferred into a 1:1 mixture of nutrient soil and vermiculite and continuously cultured in a growth chamber with a temperature of 21 ± 2 °C on a 16 h-light/8-h dark cycle. Thirty days later, propagules were transferred into square flower pots (7 × 7 cm) with the same medium. Stress treatments were performed at the six-leaf stage. For the physiological index analysis, all propagules were treated with 200 mM NaCl for 0, 1, 3, 6, 9, and 12 d. The propagules of *C. lavandulifolium* were treated with 200 mM NaCl for 12 h for the transcriptomic analysis and treated with 200 mM NaCl for 6, 24, or 48 h for the RT-PCR analysis, and the leaves were frozen in liquid nitrogen and conserved at –80 °C for RNA isolation.

Seeds of *A. thaliana* sterilized with 70% alcohol for 20 s and rinsed four times were germinated in 1/2 MS medium. After being vernalized in a refrigerator at 4 °C for 24 h, they were placed in a tissue culture room. When the roots of the seedlings had grown to 2 to 3 cm, they were transplanted to flowerpots with turf and vermiculite (v:v = 1:1) media in short-day conditions (12/12-h light/dark, 300 $\mu E \cdot m^{-2} \cdot s^{-1}$). After 1 month, the seedlings were placed in long-day conditions (16/8-h light/dark, 300 $\mu E \cdot m^{-2} \cdot s^{-1}$). The room temperature was kept at 22 ± 1 °C, and relative air humidity was 60%. *A. thaliana* bolted and flowered after 1 month, and then was used for transgenic breeding.

Physiological analyses. The method used for relative water content (RWC) determination was described in Jain and Chattopadhyay (2010). The procedure used for free proline content was based on the method described in Bates et al. (1973). Total flavonoids were estimated using a colorimetric strategy (Bao et al., 2005). Peroxidase (POD) action was measured using the method reported in Rivero et al. (2001). For chlorophyll measurement, leaves were ground in 80% chilled acetone. Then, leaves were centrifuged at 4 °C and 15,000 g_n for 5 min, the supernatant was removed, and its absorbance was measured at 663, 645, and 480 nm. Values were computed as described by Aydi et al. (2010). The malondialdehyde (MDA) content was estimated using a strategy by Heath and Packer (1968). All experiments were repeated in triplicate.

Illumina sequencing and bioinformatics investigation. In our previous study, we constructed a transcriptome database of *C. lavandulifolium* using a sequencing platform (HiSeq 2000; Illumina, Shenzhen, China). In all, 108,737 unigenes were obtained, of which 58,093 were annotated by a similarity search with known proteins (E-value < $1.00E^{-5}$) (Wang et al., 2014). For the gene expression analysis by DGE technology, total RNA was extracted from the leaves of *C. lavandulifolium* seedlings described previously (200 mM NaCl treated for 0 and 12 h) using TRIzol (Huayueyang Biotechnology, Beijing, China).

Altogether, 30 μg of total RNA was sent to the Beijing Genomics Institute organization (BGI, Shenzhen, China) for sequencing. The sequencing process was followed as described in our methods previously (Wang et al., 2014).

To identify DEGs, a rigorous algorithm to identify differential transcript accumulation between the two samples was

developed based on the method described by Audic and Claverie (1997). The false-discovery rate (FDR) was used to determine the threshold of the probability value for multiple tests. In this study, DEGs were restricted to FDR ≤ 0.001 and the absolute value of $\log_2$ ratio ≥ 1 (a 2-fold change) to judge the significance of gene expression differences.

Gene ontology (GO) and pathway enrichment analysis was performed by mapping all the DEGs to the GO (Boyle et al., 2004) and KEGG databases (Wixon and Kell, 2000). The number of DEGs involved in each GO term and pathway was calculated. By comparing these results with the assembled transcriptome of *C. lavandulifolium*, the significantly enriched pathways were identified using a $P \leq 0.05$.

Gene expression analysis of DEGs between *C.* ×*morifolium* and *C. lavandulifolium* using RT-PCR. To validate the reliability of DGE technology and RT-PCR experiments, a total of 13 candidate DEGs that were significantly increased in *C. lavandulifolium* were selected for qRT-PCR. For qRT-PCR, each reaction contained 2.0 μL of cDNA, 10 μL of SYBRGreen I (Takara Bio Inc., Shiga, Japan), and 1 μL of gene-specific primers (5.0 μM) to a final volume of 20 μL. The PCR parameters were 95 °C for 2 min, followed by 40 cycles of 95 °C for 20 s, 57 to 59 °C for 30 s, and 72 °C for 30 s. The *C. lavandulifolium* α-tubulin gene (*ClTUA*) was regarded as an internal control gene (Huang et al., 2012b). RT-PCR was used first to analysis the expression patterns of DEGs between *C.* ×*morifolium* and *C. lavandulifolium.* The PCR-amplification process and the heatmap construction methods were followed as described in our methods previously (Huang et al., 2012b).

Bioinformatics analysis, vector construction, and *A. thaliana* transformation of *ClAKT2*. The function of *ClAKT*, which was highly expressed in *C. lavandulifolium* and minimally expressed in 'Xueshan', was analyzed. Multiple sequence alignments were performed using DNAMAN (Lynnon Corp., Vaudreuil, QC, Canada). A phylogenetic tree was constructed using MEGA 5.0 software (Tamura et al., 2011) based on the neighbor joining method. The transmembrane domain of the protein was predicted based on von Heijne transmembrane prediction (von Heijne, 1992). The cDNA that was obtained using gene-specific primers (AKT-*Sal*I: TGATGTCGACATGGATCTAAAGATAG, AKT-*Bam*HI: AGAGGATCCAGGGATATCTCCT. *Sal*I site and *BamH*I site are in the box) was inserted into a pCAMBIA2301 vector. To obtain transgenic plants, the vector was transformed into the *Agrobacterium tumefaciens* strain GV3101 with liquid nitrogen treatment, and *A. thaliana* plants were transformed using the floral dip method (Clough and Bent, 1998).

Stress resistance analysis of transgenic *A. thaliana*. Seeds from the second transgenic (T_2) generation were germinated in normal 1/2 MS medium. After 10 d, they were carefully transferred to 1/2 MS medium without K^+ (1/2 MS-K), and root length was collected after 2 weeks. Seeds from the T_2 generation were germinated in 1/2 MS medium containing 100 and 200 mM NaCl (1/2 MS + 100 Na and 1/2 MS + 200 Na), and root length was collected after 3 weeks. Seeds from the T_2 generation were germinated in normal 1/2 MS medium and transferred to 1/2 MS medium without K^+ but with 50 mM NaCl (1/2 MS-K+50 Na) after 10 d, and root length was collected after 2 weeks.

Wild-type and T_2 *A. thaliana* seeds were germinated in 1/2 MS medium after cold treatment at 4 °C for 48 h. Until plant germination, they were transferred to flowerpots with turf and vermiculite (1:1 v/v) media (Dong et al., 2018). Half of them were treated with 200 mM NaCl 1 month later. After 4 d, the leaves and roots were collected for determination of Na^+ and K^+. The other half were stopped from watering at 50 d. The leaves and roots were collected for determination of Na^+ and K^+ 14 d later. The method was as follows: after the samples were stored at 80 °C for 8 h to deactivate enzymes, they were ground in an agate mortar, and 2.000 g was accurately weighed in a 125-mL Erlenmeyer flask. After they were digested in mixed liquor containing nitric acid and perchloric acid (4:1 v/v), the residual liquid was brought up to 25 mL with distilled water. The content of Na^+ and K^+ was measured by a flame atomic absorption spectrophotometer.

Results and Discussion

Salt tolerance differences in three chrysanthemum cultivars and *C. lavandulifolium*. A comparison of salt tolerance differences between three chrysanthemum cultivars (Xueshan, Xueshen, and Jinba) and *C. lavandulifolium* was conducted by physiological analyses. Six indexes were measured in seedlings after 0, 1, 3, 6, 9, or 12 d of salt treatment. RWC reflects osmotic adjustment, which is considered the most important mechanism for adaptations to abiotic stresses, such as salt, drought, and cold, in higher plants. During treatment, RWC increased after 1 d in *C. lavandulifolium*, 'Xueshen', and 'Jinba', which may have resulted from an osmotic adjustment due to osmolyte synthesis under stress, whereas the RWC of 'Xueshan' decreased. After this initial increase, the RWC of the three chrysanthemum cultivars showed a continual decrease over the 12 d (Fig. 1A), whereas in *C. lavandulifolium*, RWC showed a steep decrease up to the end of treatment (12 d).

Proline accumulation is considered one of the indicators of an adaptive response. All of the four genotypes showed greater proline content within 6 d of treatment, and this index continued to increase until the end of salt treatment. Proline accumulation in *C. lavandulifolium* and 'Jinba' were more than 2- to 2.5-fold greater than the other two cultivars (Fig. 1B). Chlorophyll content is considered the measure of the rate of photosynthesis. This index decreased with the beginning of salt treatment in 'Xueshan' and 'Xueshen' but increased in *C. lavandulifolium* and 'Jinba' under salt treatment (Fig. 1D). Salt stress significantly increased POD activity and MDA content in the leaves of *C. lavandulifolium* and 'Jinba', which was maintained until day 12, but the changes in the other two chrysanthemum cultivars showed a very slow rate of increase rate and low content under salt treatment (Fig. 1E, 1F). For flavonoids, although the level in *C. lavandulifolium* barely changed over the time course, but the specific content were more than about 2.5-fold greater than 'Xueshan' and 'Xueshen' at the end of the salt stress [12 d (Fig. 1C)]. Taken together, *C. lavandulifolium* and 'Jinba' displayed better tolerance to salt stress than the other two cultivars, whereas 'Xueshan' was a salt-sensitive cultivar, which was consistent with our previous research that the relative growth rate of 'Xueshan' decreased significantly under salt stress (Zhang et al., 2012).

Identification of DEGs. We built a transcriptome database of *C. lavandulifolium* using an Illumina HiSeq 2000 sequencing platform in our previous study. There were 108,737 unigenes that were assembled from 4-Gbp sequencing clean reads with 98.3% of the quality score of 20 (Q20) value, of which 58,093 were annotated with function-known proteins (E-value\1.00E^{-5}).

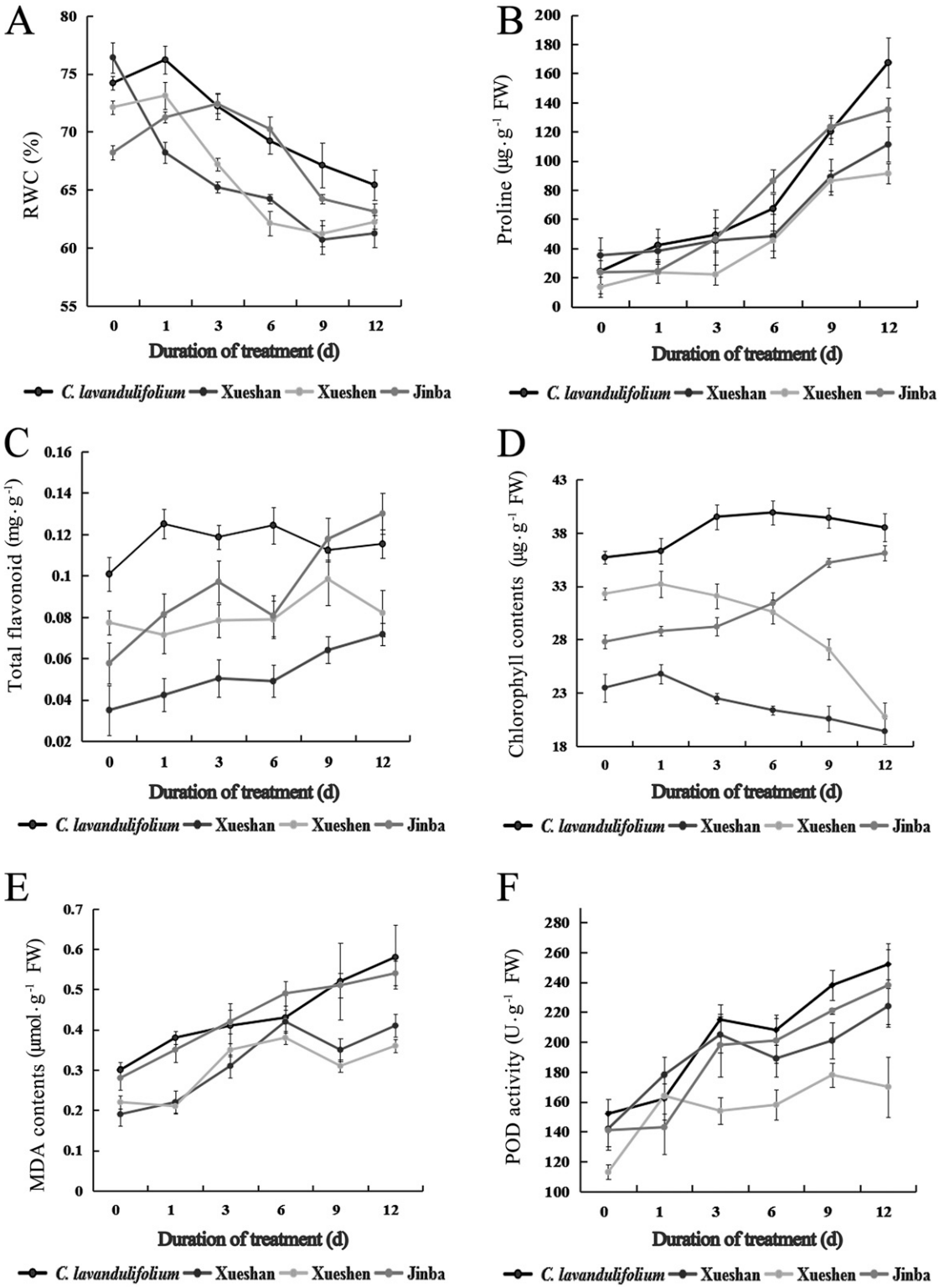

Fig. 1. Physiological response of *Chrysanthemum lavandulifolium* and *C.* ×*morifolium* 'Xueshan', 'Xueshen', and 'Jinba' leaves during salt treatment: (**A**) relative water content (RWC), (**B**) free proline content, (**C**) total flavonoids content, (**D**) chlorophyll content, (**E**) malondialdehyde (MDA) content, and (**F**) peroxidase (POD) activity.

Among these 58,093 unigenes, 19,836 were grouped into 44 functional classes using Blast2GO (Conesa et al., 2005) programming, 26,462 were mapped onto 119 KEGG pathways, and 25,565 unigenes were grouped into 25 clusters of orthologous groups (Natale et al., 2000) classifications (Wang et al., 2014). In this study, from the control [CK (seedlings were treated with clear water for 12 h)] and salt stress treatment [S1 (seedlings were treated with an equivalent amount of 200 mM NaCl for

12 h)], the updated version of the DGE method produced 591.7 and 573.9 MB, respectively (Supplemental Table 1). To explore the differently expressed genes under salt stress, the clean reads were mapped to the aforementioned *C. lavandulifolium* reference transcriptome database. In all, 4,185,231 (33.84%) and 4,013,617 (34.26%) for CK and S1 were mapped to the reference transcriptome, respectively. The coverage of unigenes was greater than 90% in the two samples, which represented 28% (24,195) and 37% (22,693) for CK and S1, individually, and the coverage was over 60%, which represented 65 and 62% for CK and S1, respectively (Fig. 2A).

Next, we measured unigene expression using the uniquely mapped DGE reads and standardized the results to the reads per kilobase of transcript per million mapped reads (RPKM). We distinguished DEGs with FDR $\leq$ 0.001 and absolute value of $\log_2$ ratio $\geq$ 1. To distinguish the critically changed unigenes, we set the two-overlap change and a probability value of under 0.05 as the cutoffs. Thus, 1952 unigenes were classified to DEGs, including 1418 that were significantly upregulated and 836 that were downregulated (Fig. 2B).

KEGG pathway enrichment and GO-term analysis of DEGs. Pathways with Q values $\leq$0.05 were chosen as significantly enriched pathways after multiple test corrections, and 32 critically enriched pathways were detected after salt treatment in *C. lavandulifolium,* including 20 pathways for which the expression of the genes was increased and 12 pathways that were downregulated (Table 1). Genes in the pathways for Phenylpropanoid biosynthesis (ko00940), Biosynthesis of secondary metabolites (ko01110), Flavonoid biosynthesis (ko00941), Plant-pathogen interaction (ko04626), Plant hormone signal transduction (ko04075), Starch and sucrose metabolism (ko00500), Metabolic pathways (ko01100), Anthocyanin biosynthesis (ko00942), Flavone and flavonol biosynthesis (ko00944), Cysteine and methionine metabolism (ko00270), Pentose and glucuronate interconversions (ko00040), and DNA replication

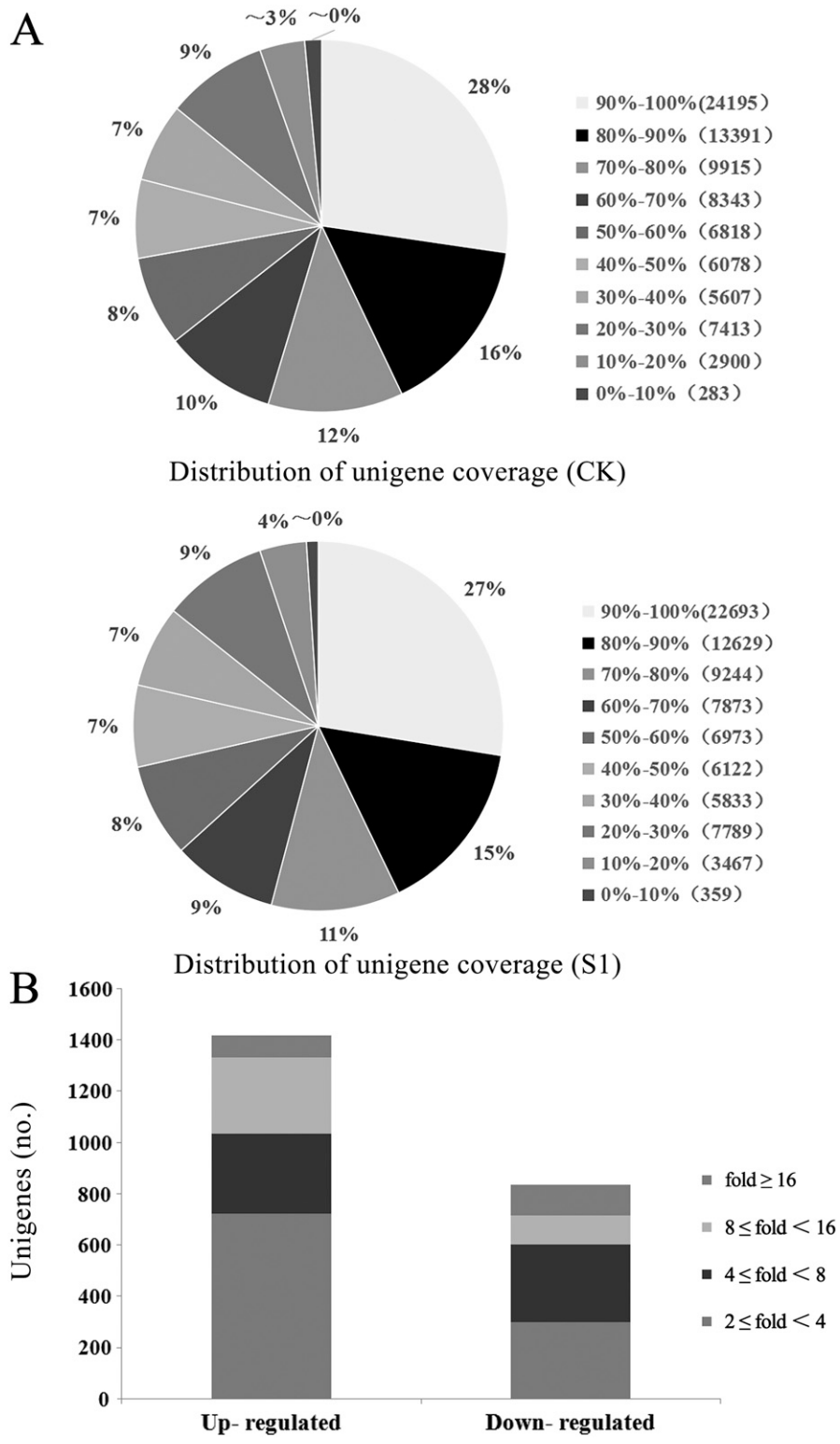

Fig. 2. (**A**) Distribution of unigene coverage in the control [CK (left)] and salt treatment samples [S1 (right)]. Different colors represent the percentage of different proportions of unigene coverage. The number of unigenes is indicated in parentheses. (**B**) Statistics of differentially expressed genes (DEGs). Different color column represent DEGs within diverse fold changes (Fold = Na200_RPKM/CK_RPKM); CK = seedlings were treated with clear water for 12 h; S1 = seedlings were treated with an equivalent amount of 200 mM NaCl for 12 h; RPKM = the reads per kilobase of transcript per million mapped reads.

Table 1. The significantly enriched Kyoto Encyclopedia of Genes and Genomes [KEGG (Wixon and Kell, 2000)] pathways in the differentially expressed genes (DEGs) commonly regulated by salt stress.

Pathway	DEGs [no. (%)][z]	Unigenes [no. (%)][y]	Corrected *P* value[x]	Pathway ID[w]
Up-regulated				
Phenylpropanoid biosynthesis	65 (5.39)	794 (3.00)	3.47628E-19	ko00940
Biosynthesis of secondary metabolites	192 (15.86)	3462 (13.08)	1.42219E-08	ko01110
Flavonoid biosynthesis	45 (3.77)	426 (1.61)	2.56856E-09	ko00941
Plant–pathogen interaction	149 (12.33)	2138 (8.08)	1.15666E-24	ko04626
Plant hormone signal transduction				ko04075
Starch and sucrose metabolism	58 (4.77)	823 (3.11)	2.96278E-10	ko00500
Metabolic pathways	306 (25.33)	6270 (23.70)	0.004407798	ko01100
Anthocyanin biosynthesis	38 (3.20)	39 (0.15)	0.001271844	ko00942
Flavone and flavonol biosynthesis	28 (2.33)	176 (0.67)	1.9036E-07	ko00944
Cysteine and methionine metabolism	30 (2.47)	401 (1.52)	2.89153E-07	ko00270
Pentose and glucuronate interconversions	19 (1.56)	218 (0.82)	2.18001E-07	ko00040
DNA replication	15 (1.26)	203 (0.77)	0.000176454	ko03030
ABC transporters	20 (1.68)	311 (1.18)	0.001244894	ko02010
Phenylalanine metabolism	26 (2.20)	352 (1.33)	6.76907E-07	ko00360
Phosphonate and phosphinate metabolism				
Propanoate metabolism	9 (0.74)	191 (0.72)	0.022853249	ko00640
Arginine and proline metabolism	16 (1.28)	252 (0.95)	0.000168745	
Polycyclic aromatic hydrocarbon degradation			0.000716149	ko00624
Stilbenoid, diarylheptanoid, and gingerol biosynthesis	37 (3.06)	557 (2.10)	7.08228E-06	
Fatty acid metabolism	13 (1.06)	263 (0.99)	0.01166959	ko00071
Down-regulated				
Metabolic pathways	92 (12.41)	6270 (23.70)	0.004407798	ko01100
Biosynthesis of secondary metabolites	31 (4.12)	3462 (13.08)	1.42219E-08	ko01110
Fatty acid metabolism	26 (3.56)	263 (0.99)	0.01166959	ko00071
Ribosome	41 (5.58)	645 (2.44)	6.89099E-07	
Tryptophan metabolism	9 (1.19)	274 (1.04)	2.63541E-06	
Nitrogen metabolism	12 (1.72)	242 (0.91)	3.67784E-09	ko00910
Aminobenzoate degradation			0.03884857	ko00627
Bisphenol degradation			0.01084123	ko00363
Beta-alanine metabolism	4 (0.54)	128 (0.48)	0.3102526	ko00410
Zeatin biosynthesis	13 (1.73)	259 (0.98)	7.83477E-07	ko00908

[z]Number of DEGs assigned to certain KEGG pathway.
[y]Number of all reference unigenes assigned to certain KEGG pathway.
[x]Significantly enriched KEGG pathways were determined using a corrected $P \leq 0.05$.
[w]Identification.

(ko03030) were specifically enriched in the upregulated DEGs. Unigenes involved in Fatty acid metabolism (ko00071), Ribosome (ko03010), Nitrogen metabolism (ko00910), and Tryptophan metabolism (ko00380) were only enriched in the downregulated DEGs, which demonstrated that all the major basal metabolic processes, including protein synthesis, energy, and lipid metabolism, and photosynthesis were severely affected by salt stress.

The DEGs were annotated using Blast2GO programming against the NCBI nr protein database with a cut-off E-value of 10–10 and assigned with GO terms to biological processes, cellular components and molecular functions. From 1952 DEGs, 1454 unigenes exhibited significant BLAST hits (73.5%), and the remaining 26.5% did not exhibit any arrangements. Figure 3 shows how many genes are allocated to no fewer than one GO term and assembled into three primary GO classifications: biological process (A), cellular component (B), or molecular function (C). Among these unigenes, 758 DEGs were identified in the molecular function class of GO annotation. The top hits included genes involved in anion transmembrane transporter activity (18/23 unigenes), antioxidant activity (20/24 unigenes), transmembrane transporter activity (14/17 unigenes), oxidoreductase activity (50/67 unigenes), molecular transducer activity (47/63 unigenes), and signal transducer activity (21/28 unigenes). In the cellular component category, the top hits were genes found to be active in the extracellular region (19/21 unigenes), vacuole (20/25 unigenes), macromolecular complex (15/19 unigenes), organelle lumen (11/15 unigenes), anchored to the membrane (36/51 unigenes), vesicle (31/45 unigenes), organelle inner membrane (6/9 unigenes), cell wall (25/38 unigenes), and cytoplasmic vesicle (24/37 unigenes). For the biological process category, 901 unigenes were assigned GO terms. The top hits included genes in the lipid biosynthetic process (18/21 unigenes), the proline metabolic process (6/7 unigenes), the L-phenylalanine metabolic process (18/22 unigenes), response to organic substance (17/21 unigenes), protein amino acid phosphorylation (4/5 unigenes), signal transduction (27/34 unigenes), secondary metabolic process (20/26 unigenes), transport (38/51 unigenes), and activity of transcription regulators (31/46 unigenes).

To confirm the expression pattern reliability of the high-throughput sequencing technology, 12 genes induced by salt

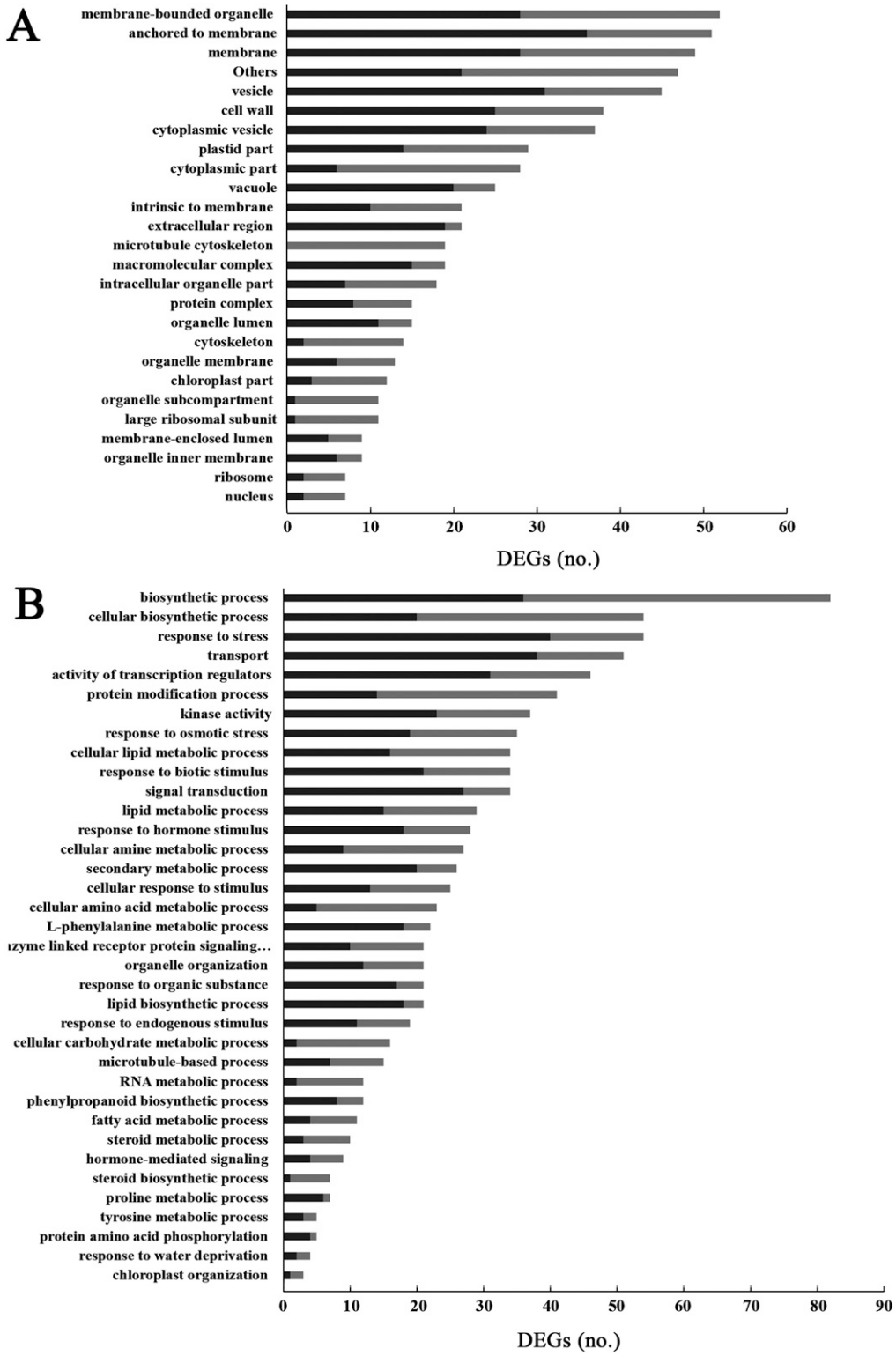

Fig. 3. Summary of differentially expressed genes (DEGs) using Blast2GO (Conesa et al., 2005). DEGs were classified into three main gene ontology [GO (Boyle et al., 2004)] annotations: cellular component (**A**), biological processes (**B**), and molecular functions (**C**). There are 36 GO terms for biological processes, 29 GO for molecular function, and 37 GO for cellular component.

stress were chosen for validation by qRT-PCR. The results demonstrated that the expression of the tested unigenes was consistent with the DGE data (Fig. 4), indicating that the high-throughput sequencing technology used in the present study could provide biological relevant, repeatable, and reliable results.

Classification of salt-response transcripts. A rigorous algorithm (FDR ≤ 0.001, $\log_2$ ratio ≥ 1) of the RPKM-derived

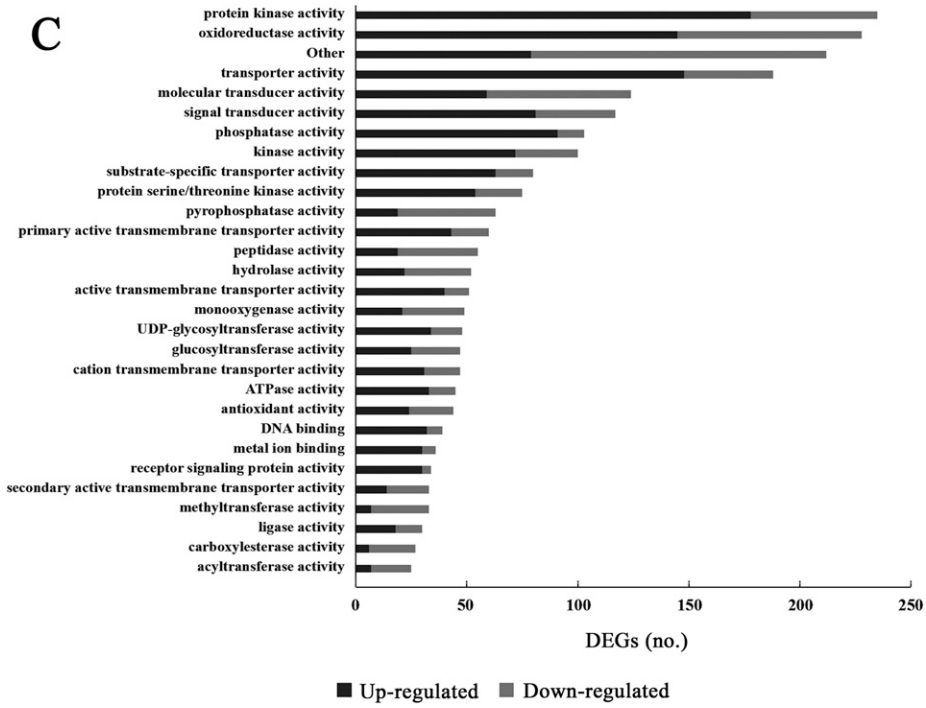

Fig. 3. (continued).

read counts was carried out to identify DEGs that differed between the two samples. At 12 h, the expression of 1418 genes were induced, and the expression 836 genes were inhibited. Most broadly, the salt-response transcripts could be divided into regulators and effectors (Jiang and Deyholos, 2006). According to the GO and KEGG enrichment analysis, the most prominent effectors of the NaCl stress response genes in *C. lavandulifolium* were the genes involved in the ROS-scavenging system, ion transport, biosynthesis of secondary metabolites, and osmoprotectant production, whereas the major classes of regulators were signal transduction components, hormone-related genes, and transcription factors (TFs). Supplemental Tables 2 – 5 show groups of the aforementioned related genes. The supplemental tables also include the number of unigenes belonging to each category that were up- or downregulated more than 2- and 5-fold.

Signal transduction components and TFs. More than 60 DEGs encoding signal transduction kinases were significantly differentially expressed in *C. lavandulifolium* after 12 h of salt treatment (Supplemental Table 2). In response to salt stress, early signaling events in plants include increased flux of Ca^{2+} into the cytosol, activation of mitogen-activated protein kinases (MAPKs), and ABA-related genes (Golldack et al., 2014). A total of 39 genes belonging to the calcium signaling category were detected, such as calmodulin 2, calreticulin 3, calmodulin-like proteins, calcium-dependent protein kinases, CBL-interacting protein kinases (CIPKs), and CBL-interacting serine/threonine-protein kinases (Steinhorst and Kudla, 2013). In *C. lavandulifolium*, *CBLs* (*calcineurin B-like genes*) and *CIPKs* were induced, especially the 13 *CIPK* genes, in which four changed 5-fold after salt treatment. These two kinase families form a dynamic complex to plant responses to many environmental signals and in regulating ion fluxes under salt stress (Yu et al., 2014). In *A. thaliana*, CBL4 (orthologs of Unigene104333_CL32) (salt overly sensitively 3, SOS3) interacts with CIPK24 (SOS2, orthologs of Unigene82254_CL32), and this interaction activates the plasma membrane-localized SOS1 and vacuolar H^+-ATPase to promote salt tolerance (Liu et al., 2015). The CBL10-CIPK24 (orthologs of Unigene91258_CL32 and Unigene82254_CL32) complex is associated with vacuolar compartments and functions in protecting shoots from salt stress (Kim et al., 2007), whereas the interaction of CBL1 or CBL9 (orthologs of Unigene91258_CL32) with CIPK23 phosphorylates and activates the K^+ channel AKT1 to modulate K^+ homeostasis (Grefen and Blatt, 2012).

For other signal transduction genes, solid expression of 18 DEGs that belonged to the MAPK pathway was detected. The MAPK cascade is composed of no fewer than three protein kinases, a mitogen-activated protein kinase kinase kinase (MAPKKK), a mitogen-activated protein kinase kinase, and a MAPK (MPK), which activate each other in a successive way by means of phosphorylation (Cristina et al., 2010). Salt stress was found to rapidly initiate the activation of MAPK pathway components, such as *ZmMPK3*, *5*, and *ZmSIMK1* in *Zea mays* (Ding et al., 2013) and *AtMPK3*, *4*, and *6* in *A. thaliana* (Andreasson and Ellis, 2010).

ABA-independent and -dependent pathways regulate the expression of cascades of abiotic stress response genes (Yoshida et al., 2014). In *A. thaliana*, ≈10% of all genes were controlled by ABA. ABA is derived from carotenoids by 9-cis-epoxycarotenoid dioxygenase (NCED). In *A. thaliana*, PYR/RCAR/PYL family proteins perceive and bind to protein phosphatase 2C (PP2C) A group proteins in the presence of ABA. Subclass III SNF1-related protein kinase 2 (SnRK2) is then discharged from PP2C-dependent negative regulation, permitting the initiated SnRK2s to phosphorylate downstream genes, such as ABFs (ABA-responsive element factors) (Park

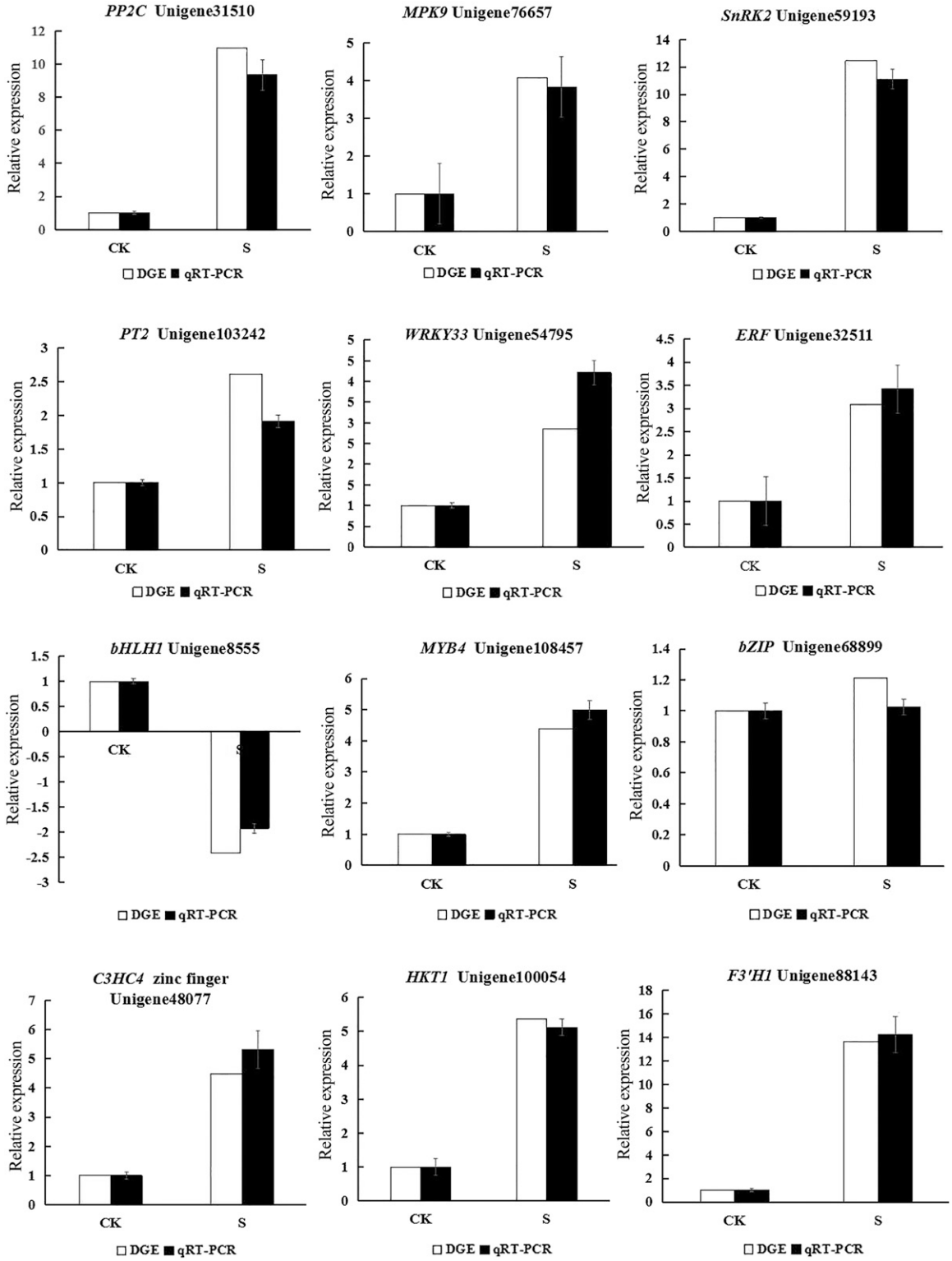

Fig. 4. Expression ratios of the 12 differentially expressed genes (DEGs) assessed by both digital gene expression (DGE) and quantitative real-time polymerase chain reaction (qRT-PCR) validation. PP2C = protein phosphatase 2C; MPK9 = MAP Kinase 9; SnRK2 = SNF1-related protein kinase 2; PT2 = phosphate transporter 2; ERF = ethylene-responsive transcription factor; bHLH1 = basic helix-loop-helix 1; MYB4 = myeloblastosis 4; bZIP = basic leucine zipper; C3HC4 = C3HC4 type zinc finger; HKT1 = high-affinity K^+ transporter 1; F3′H1 = flavonoid 3′-hydroxylase.

et al., 2009; Raghavendra et al., 2010; Wang et al., 2018b). In *C. lavandulifolium*, expression of orthologs of *PYL* (Unigene97951_CL32, PP2C (Unigene94148_CL32), SnRK2s (Unigene101215_CL32, Unigene59193_CL32), and NCED all showed strong increases under salt stress, indicating that control of that ABA signal is conserved among plant species and plays a vital role in salt-response processes in *C. lavandulifolium*.

In *C. lavandulifolium*, 185 TFs in 13 TF families were isolated, such as *AP2/EREBP*, *MYB*, *NAC*, *WRKY*, and *bHLH* families (Supplemental Table 3). Our previous report showed that at least 17 *NAC* genes responded to salt in *C. lavandulifolium*, and 10 responded to at least four types of stresses (Huang et al., 2012b). The abundance of 33 *NAC* genes showed strong changes in *A. thaliana* under salt treatment (Jiang and Deyholos, 2006), and 11 melon *NAC* (*CmNAC*) genes from group IV identified in the *Cucumis melo* genome were induced in melon seedling roots by salt stress (Wei et al., 2016). WRKY is another vital TF that regulates both biotic and abiotic stresses. Eighteen *AtWRKYs*, 15 *TcWRKYs*, and 26 *GhWRKYs* were induced by salt (Chen et al., 2012). In *C. lavandulifolium*, 13 *WRKYs* were upregulated, and two members, Unigene104646_CL32 and Unigene64406_CL32, orthologs of *AtWRKY25* and *AtWRKY33*, were significantly increased. In *A. thaliana*, these genes play regulatory roles under salt and drought stress responses, and they might act as positive regulators in mediating plant responses to ABA (Jiang and Deyholos, 2009).

Ion transport genes play a key role in salt stress responses in *C. lavandulifolium*. Various reports have shown that numerous water, ion, and metal transporters may work during salt stress. In *C. lavandulifolium*, 115 DEGs identified have high identity with transporters, such as the Na^+/H^+ antiporter (NHX), vacuolar-type proton ATPase (VAP), *A. thaliana* K^+ transporter (AKT), aquaporin, and ABC transporters (Supplemental Table 4). VATPase and vacuolar NHXs function together in sequestering Na^+ in vacuoles in salt treatment (Bassil and Blumwald, 2014), and in numerous halophytes, high transcriptional levels of these two kinds of genes were detected (Silva and Gerós, 2009). Increased V-ATPase activity could improve salt tolerance in transgenic crops (Dabbous et al., 2017; Kirsch et al., 1996; Pasapula et al., 2011). In *C. lavandulifolium*, greater transcript levels of V-ATPase were observed among 31 V-ATPase unigenes, including 10 P-type H^+-ATPase and 16 V-type H^+ATPase and V-type H^+-pyrophosphatases. Among 10 Na^+ efflux unigenes, the *SOS1* gene (Unigene102112_CL32) showed moderate transcript levels, whereas four (Unigene91877_CL32, Unigene102112_CL32, Unigene84735_CL32, and Unigene81673_CL32) were highly abundant and all showed high homology to the *NHX2* of *A. thaliana*, demonstrating that these AtNHX2-like proteins play a vital role in mitigating or avoiding the harmful impacts of high Na^+ levels, which have been reported in *A. thaliana* (Yokoi et al., 2002). Moreover, the maintenance of high intracellular K^+/Na^+ ratios is important to avoid Na^+ poisoning. Several genes that have high similarity with potassium transport proteins were identified, but only *AKT1* (Unigene1555_CL32) and two *HKT* (Unigene100054_CL32, Unigene107272_CL32) genes were upregulated, which may function in ion transport and are strongly induced during salt stress to maintain or reset homeostasis in the cytoplasm.

ROS response network and osmoprotectants. When subjected to the abiotic stress, an intense increase in ROS production in plants is expected, which are capable of perturbing cellular redox homeostasis and oxidative impairment to cellular structures and ultimately leading to the death of the cell (Baxter et al., 2014). ROS are generated by *RBOH* genes in a Ca^{2+}-dependent approach (Suzuki et al., 2011). In the present study, significant upregulation of 2 *RBOH* unigenes (Unigene27241_CL32, Unigene12799_CL32) was observed responding to the salt. The *MAPK* cascade *MEKK1-MKK2-MPK4/6*, in addition to *bHLH92* and *WRKY33*, were also participates in ROS signaling through targeting both the peroxidases and glutathione-S-transferases (Jiang and Deyholos, 2009; Zhang et al., 2011). We noticed that upregulation of the transcript level of a *MAPK* (Unigene81764_CL32), 2 *MAPKKKs* (Unigene98646_CL32 and Unigene35698_CL32), and *WRKY33* (Unigene84179_CL32) were all increased more than 2-fold under salt stress, indicated that these orthologs constituted key roles of the ROS signal transduction pathway as they are involved in the mediation of salt stress in *C. lavandulifolium*. Among the ROS scavenging-related enzymes gene families, most *APX*, *SOD*, *GST*, and *GRX* genes were expressed strongly under salt stress (Supplemental Table 5). This result also was consistent with the physiological results that MDA content and POD activity were increased under salt treatment, which indicated that these enzymes may be the main scavengers of ROS in salt stress in *C. lavandulifolium*.

All unigenes in the proline biosynthetic pathway were increased by salt stress in *C. lavandulifolium*, particularly those encoding the key compound pyrroline-5-carboxylate synthetases (P5CS, Unigene88101_CL32). Conversely, unigenes encoding proline dehydrogenase (*PDH*, Unigene93330_CL32), the key enzyme in proline degradation, were downregulated. Proline transport also is indispensable in plant responses to stress and normal growth and development (Sharma et al., 2011; Zarattini and Forlani, 2017). We found four unigenes encoding proline transporter, which all had significantly increased expression (Supplemental Table 5). Integrated physiological analysis showed that *C. lavandulifolium* accumulated greater free proline content after salt treatment, indicating that proline pathways in *C. lavandulifolium* play a significant role in response to stress.

Flavonoid genes are important for salt tolerance in *C. lavandulifolium*. Flavonoids have antioxidant activity and are of prime significance for plant defense against pathogens and ultraviolet stress (Brunetti et al., 2013). Yuan et al. (2015) revealed that drought induced the expression of several flavonoid biosynthesis genes in *Scutellaria baicalensis* roots. In *Ammopiptanthus mongolicus*, flavonoid biosynthesis genes were enriched upregulated GO terms by both low temperature and dehydration (Wu et al., 2014). Genes encoding almost all the flavonoid biosynthesis enzymes were highly expressed in *C. lavandulifolium* seedlings under normal conditions and then significantly increased by salt stresses (Supplemental Table 4). Furthermore, three differently expressed genes encoding MYB TFs belonged to subfamilies 4 and 6 of the *MYB* family (Unigene108457_CL32, Unigene63267_CL32, and Unigene85476_CL32) were observed. Combined with the results of physiological analyses, it is very clear that a high level of flavonoids could protect *C. lavandulifolium* cells from abiotic stresses.

Comparative gene expression analysis of DEGs in *C. lavandulifolium* and *C.* ×*morifolium* 'Xueshan'. From our physical analyses, we can conclude that *C. lavandulifolium* and 'Jinba' displayed better tolerance to salt stress than the other two cultivars, whereas 'Xueshan' was a salt-sensitive cultivar. To investigate the candidate genes that contribute to salt tolerance in *C. lavandulifolium*, comparative gene expression analysis by RT-PCR was used to compare the transcriptional levels of DEGs in *C. lavandulifolium* and *C.* ×*morifolium*

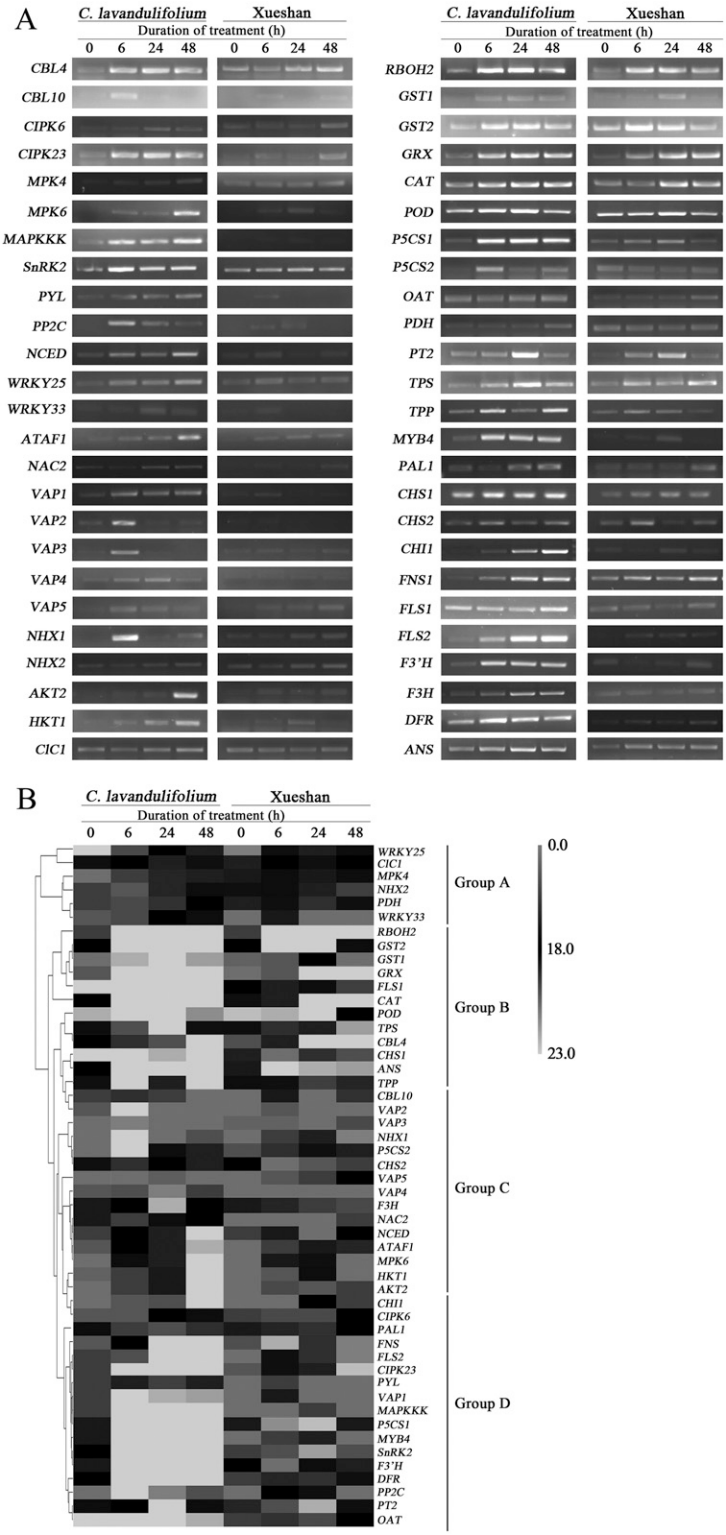

Fig. 5. (**A**) Comparative gene expression analysis by reverse transcription polymerase chain reaction was used to compare the transcriptional levels of 50 key salt-responsive genes in *Chrysanthemum lavandulifolium* and *C.* ×*morifolium* 'Xueshan' under salt treatment. (**B**) Heat map representation for expression of the genes. CBL = calcineurin B-like; CIPK = CBL-interacting protein kinase; MPK = MAP kinase; MAPKKK = mitogen-activated protein kinase kinase kinase; SnRK = SNF1-related protein kinase; PYL = abscisic acid receptor PYL; PP2C = protein phosphatase 2C; NCED = 9-cis-epoxycarotenoid dioxygenase; NAC = NAM, ATAF1/2, CUC2; VAP = vacuolar-type proton ATPase; NHX = Na^+/H^+ antiporter; AKT = *Arabidopsis thaliana* K^+ transporter; HKT = high-affinity K^+ transporter; ClC = chloride channel; RBOH = respiratory burst oxidase homologue; GST = glutathione-S-transferases; GRX = glutaredoxin; CAT = catalase; POD = peroxidase; P5CS = pyrroline-5-carboxylate synthetase; OAT = ornithine aminotransferase; PDH = phosphate dehydrogenase; PT2 = phosphate transporter 2; TPS = terpenoid synthase; TPP = trehalose-6-phosphatase; MYB = myeloblastosis; PAL = phenylalanine ammonia-lyase; CHS = chalcone synthase; CHI = chalcone isomerase; FNS = flavone synthase; FLS = flavonol synthase; F3′H = flavonoid 3′-hydroxylase; F3H = flavonoid 3-hydroxylase; DFR = dihydroflavonol 4-reductase; ANS = anthocyanidin synthase.

'Xueshan'. From the aforementioned analysis, we can see that genes involved in ion transport, flavonoid biosynthesis, proline pathways, trehalose pathways, the ROS network, signal transduction, and TFs play important roles in salt response in *C. lavandulifolium.* Combined with our results and literature reports, we chose the following 50 genes for the RT-PCR and cluster analysis: *CBL4*, *CBL10*, *CIPK6*, *CIPK23*, *MPK4*, *MPK6*, *MAPKKK*, *SnRK2*, *PYL*, *PP2C*, *NCED*, *WRKY25*, *WRKY33*, *ATAF1*, *NAC2*, *VAP1*, *VAP2*, *VAP3*, *VAP4*, *VAP5*, *NHX1*, *NHX2*, *AKT2*, *HKT1*, *ClC1*, *RBOH2*, *GST1*, *GST2*, *GRX*, *CAT*, *POD*, *P5CS1*, *P5CS2*, *OAT*, *PDH*, *PT2*, *TPS*, *TPP*, *MYB4*, *PAL1*, *CHS1*, *CHS2*, *CHI1*, *FNS1*, *FLS1*, *FLS2*, *F3'H*, *F3H*, *DFR*, and *ANS*. We believe that analysis of these genes in genotypes with different salt tolerance is useful for isolating the node factor.

From the RT-PCR and cluster analysis (Fig. 5), we can see that the expression patterns of DEGs under salt treatment could be divided into four groups after clustering (Groups A–D), which contained 6, 12, 15, and 17 genes, respectively. In group A and B, all these DEGs were induced by salt in *C. lavandulifolium* and *C. morifolium.* There were no differences in these genes between *C. lavandulifolium* and *C. ×morifolium* 'Xueshan' over the whole experimental period. These genes mainly include the trehalose and ROS pathway genes, suggesting that

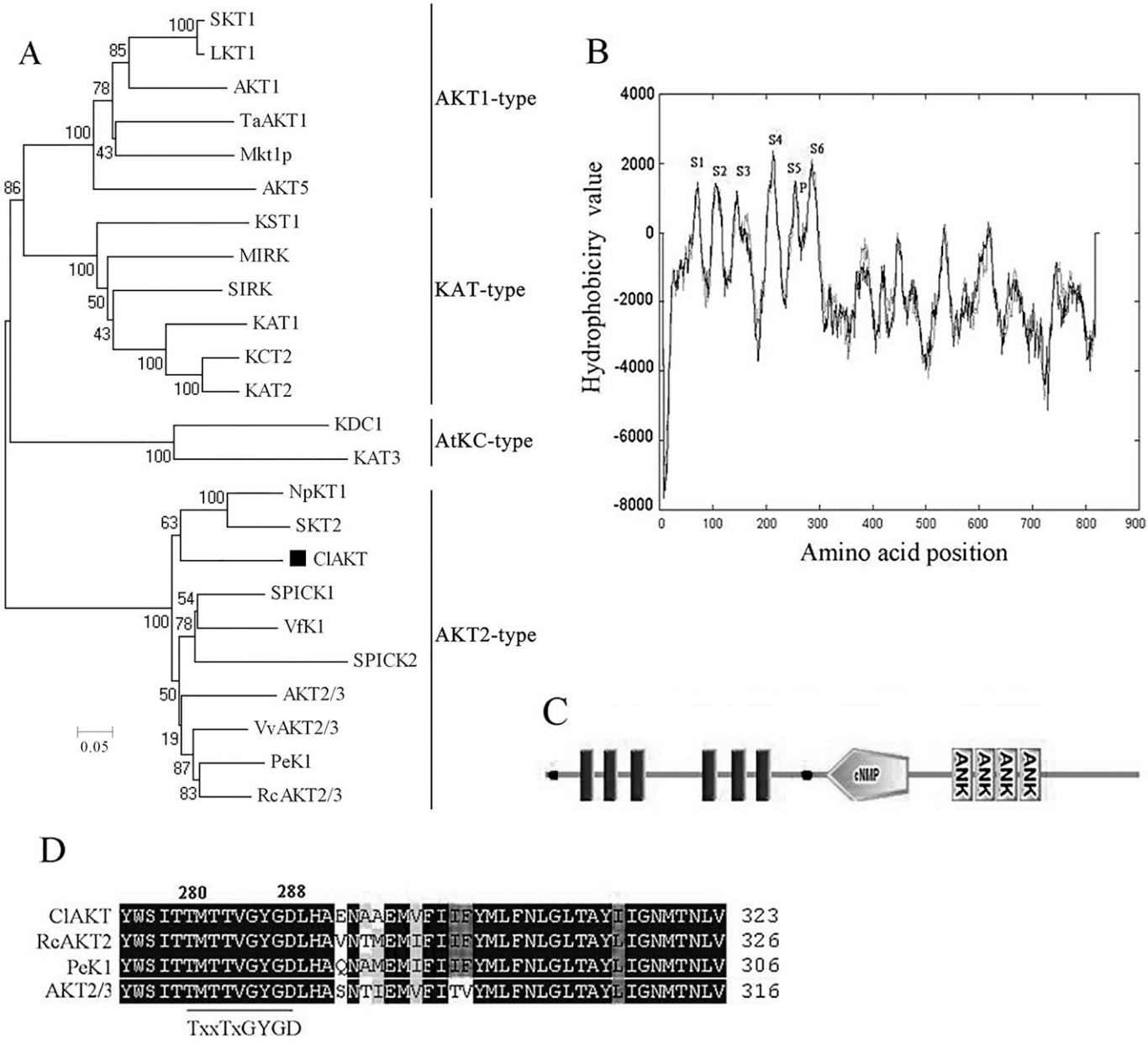

Fig. 6. Bioinformation analysis of *ClAKT2*: (**A**) phylogenetic analysis and subfamilies classification; (**B**) transmembrane domains analysis of ClAKT (S represents the transmembrane domains); (**C**) transmembrane domains analysis of ClAKT (black rectangle represents the transmembrane domains and black points represent the anchor site); (**D**) comparison of the deduced amino acid sequence of ClAKT with its homologs (underline means the TxxTxGYGD motif of plants K^+ channels). SKT1, CAA60016; LKT1, CAA65254; AKT1, NP_180233; TaAKT1, AAF36832; MKT1, AAF81249; SPIK, NP_180131; AKT6, NP_194976; MIRK, AAZ66349; SIRK, AAL09479; KST1, CAA56175; KAT1, NP_199436; KAT2, NP_193563; KCT2, AAX19659; NpKT1, BAA84085; SKT2, CAA70870; PTK2, CAC05489; AKT2, NP_567651; SPICK2, AAD39492; VfK1, CAA71598; SPICK1, AAD16278; AtKC1, NP_194991; KDC1, CAB62555.

these genes were important for salt adaptation in the genus *Chrysanthemum*. Group C contained 15 genes, which were induced quickly in *C. lavandulifolium* but slowly in 'Xueshan'. These genes included mainly the signal-transduction, transporters, and TF genes, such as *PP2C*, *PYL*, *SnRK2*, and NCED, which were the main components of the ABA-dependent pathway and were upregulated in short-term salt exposure in *C. lavandulifolium*, but in 'Xueshan', the transcriptional peak appears at 12 h and the transcript level of *AKT*, *NHXs*, *VAPs*, and SOS systems (*CBL4*, *CBL10*, and *CIPK23*) were earlier for *C. lavandulifolium* than 'Xuanshan' under salt stress. Group D contained 17 genes, which included 12 genes mainly involved in flavonoid biosynthesis and proline pathways. These genes were upregulated for both genotypes over the whole experimental period, with a greater increase for *C. lavandulifolium* vs. 'Xuanshan'.

Expression pattern and bioinformatic analysis of *ClAKT*. The damage to plants caused by salt stress is mainly reflected in two ways: ion toxicity and osmotic stress (Zhu, 2003). The toxicity of ions is reflected in the excess of Na^+ to replace K^+, which is necessary for plant growth. Therefore, a high K^+/Na^+ ratio maintained in the plant cytoplasm is essential for normal cell functioning. Two major factors that maintain intracellular K^+/Na^+ ratios are exporting Na^+ out of the cell and compartmentalizing Na^+ in vacuoles and alleviating potassium starvation caused by salt stress. The former is completed by the SOS signaling pathway and a large number of tonoplast-localized Na^+/H^+ exchangers, whereas the acquisition, accumulation, and distribution of K^+ in plant cells are accomplished by different K^+ transporters (Deinlein et al., 2014). The first K^+ transporter found in plants was KAT1 and AKT1 in *A. thaliana* (Lagarde et al., 1996; Sutter et al., 2006). In this study, the expression pattern and bioinformatics analysis of a potassium channel gene *ClAKT2* in response to salt stress in *C. lavandulifolium* was performed. The expression results showed that *ClAKT2* is highly expressed in leaves of *C. lavandulifolium* but is low in 'Xueshan'. Bioinformatics analysis revealed that the N-terminal of the AKT protein has six strong transmembrane domains, and the C-terminal hydrophobic region contains four Ankyrin repeats. The cyclic nucleotide-monophosphate binding domain consisted of 152 amino acid residues. In addition, a new result demonstrated that a highly hydrophobic region (1–55 amino acids) at the N-terminus of ClAKT2 protein, which has not been reported in AKT proteins in other plants. The phylogenetic tree combined with the classification of K^+ channel genes by Gambale and Uozumi (2006) indicates that the *ClAKT* belongs to the AKT2-type subgene family (Fig. 6).

Salt tolerance analysis of ClAKT2 transgenic *A. thaliana*. *AKT1* is present in the roots of *A. thaliana* and is responsible for participating in the absorption and transport of K^+ (Lagarde et al., 1996). At present, there are many experiments to prove that the transgenic *AKT1* gene can enhance plant salt tolerance and improve K^+ utilization efficiency (Ardie et al., 2010; Liu et al., 2015). *AKT2* is mainly localized in phloem cells, and potassium starvation and exogenous ABA can increase its expression level (Deeken et al., 2002; Pilot et al., 2003a, 2003b). However, compared with *AKT1*, there are few studies on the function of *AKT2*. Therefore, the full length of *AKT2* was amplified and then used for transgenic studies.

As Fig. 7 shows, the root growth of *ClAKT*-transgenic *A. thaliana* is slightly greater than that of wild type *A. thaliana* under normal cultivation conditions. Under low salt stress, the phenotypes of transgenic plants were similar to nontransgenic

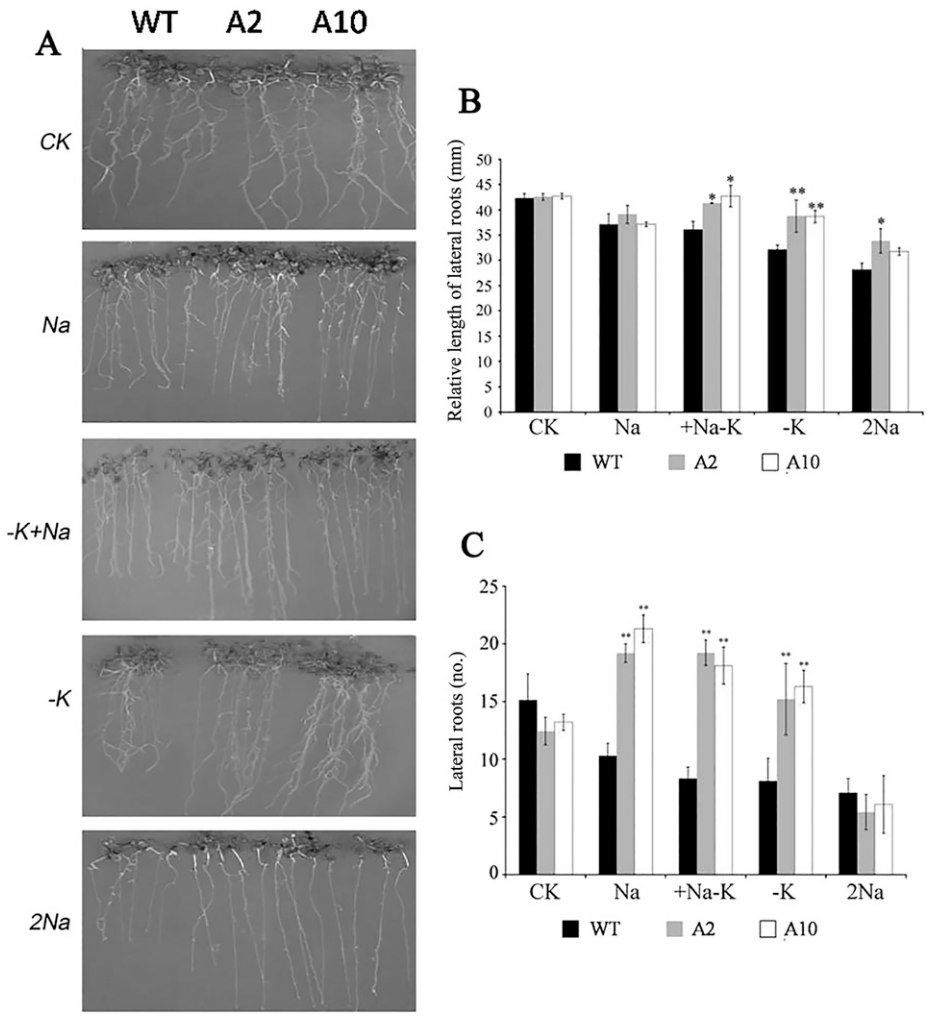

Fig. 7. Phenotype of wild-type (WT) and *ClAKT2*-expressing *Arabidopsis thaliana*. (**A**) seedlings of WT and A2 and A10 were germinated on a 1/2 Murashige and Skoog (MS) agar plate supplemented with different abiotic stresses. The relative root (**B**) length and (**C**) numbers of lateral root of WT and *35S-ClAKT* seedlings treated by different abiotic stresses in comparison with control seedlings. A2 = *35S-ClAKT* transgenic *A. thaliana* line 2; A10 = *35S-ClAKT* transgenic *A. thaliana* line 10. CK = 1/2 MS, Na: 1/2 MS+100 Na, +Na-K: 1/2 MS-K+50 Na, –K: 1/2 MS-K, 2Na: 1/2 MS+200 Na.

plants, whereas the root growth of transgenic plants is significantly greater than that of wild-type plants in the absence of potassium (–K+Na, –K). Interestingly, although the phenotypes of transgenic plants and wild-type *A. thaliana* are similar at low salt concentrations, the root growth and survival rate of *ClAKT*-transgenic *A. thaliana* is significantly greater than that of wild-type *A. Thaliana* at high salt concentrations. In addition, in the low-salt concentration treatment group, the number of lateral roots was significantly increased in transgenic plants compared with wild-type plants.

After 4 d of salt stress treatment, the Na^+ and K^+ in the leaves and roots of wild-type and transgenic plants showed that the roots of the transgenic plants significantly absorbed K^+ and excreted Na^+, whereas the leaves significantly absorbed K^+, but the amount of K^+ absorption did not change significantly (Fig. 8A and B). Furthermore, transgenic plants significantly increased K^+ uptake in roots and leaves under drought stress (Fig. 8C and D).

The results of this study indicating that *ClAKT2*-transgenic *A. thaliana* can accumulate K^+ in leaves and roots is consistent

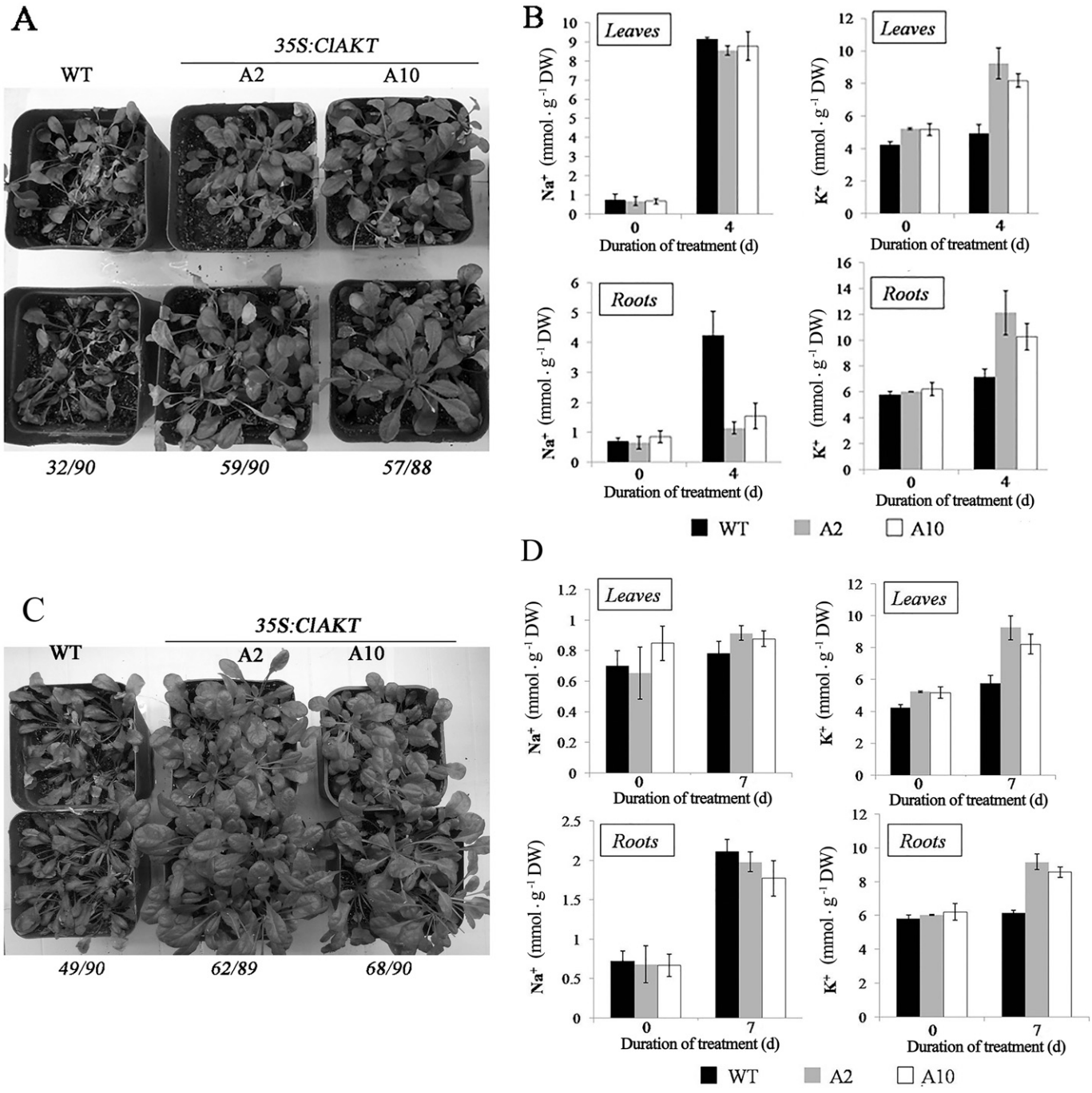

Fig. 8. Effect of *ClAKT2* overexpression on growth of *Arabidopsis thaliana* (**A**) and Na^+, K^+ content in different plant organs (**B**) under salt treatment. Effect of *ClAKT* overexpression on growth of *A. thaliana* (**C**) and Na^+, K^+ content in different plant organs (**D**) under drought treatment. The numbers on the x-axis of **A** and **C** are these plants survival numbers. WT = wild type; A2 = *35S-ClAKT* transgenic *A. thaliana* line 2; A10 = *35S-ClAKT* transgenic *A. thaliana* line 10.

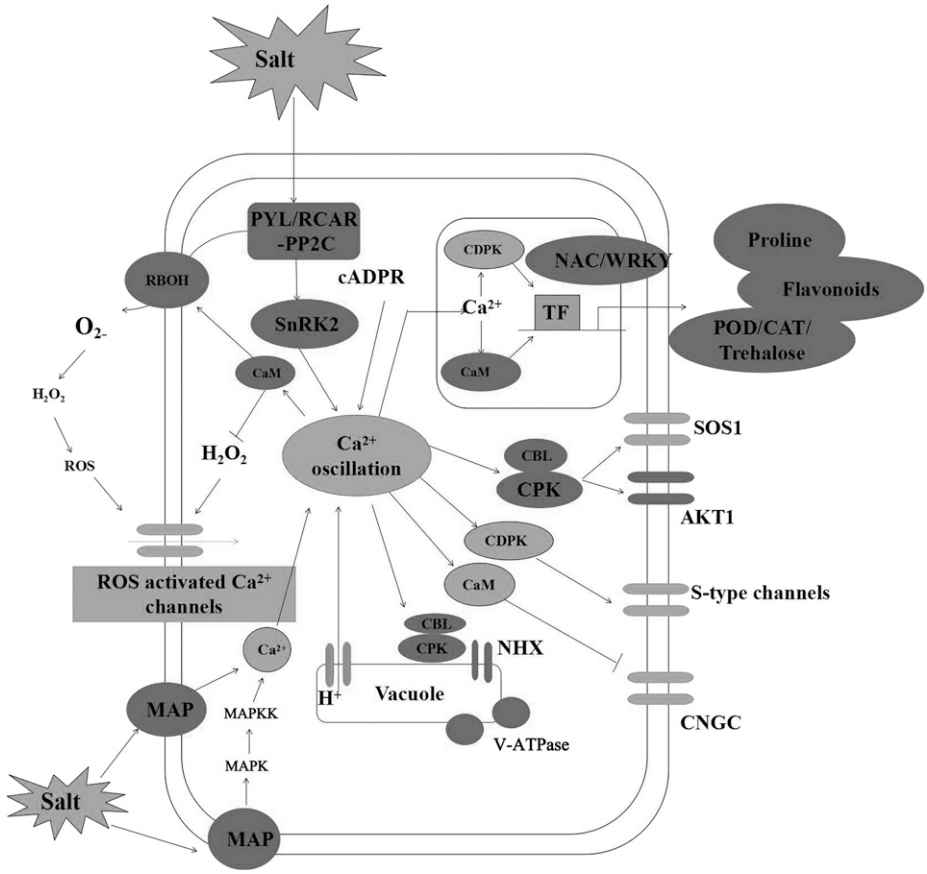

Fig. 9. A proposed model revealing the potential mechanism of salt stress response in *Chrysanthemum lavandulifolium*. PYL = pyrabactin resistance 1-like; RCAR-PP2C = RCAR-protein phosphatase 2C; cADPR = cyclic adenosine diphosphate (ADP)-ribose; SnRK2 = SNF1-related protein kinase 2; RBOH = respiratory burst oxidase homologue; CaM = calmodulin; CDPK = calcium-dependent protein kinase; NAC = NAM, ATAF1/2, CUC2; TF = transcription factors; POD = peroxidase; CAT = catalase; CBL = calcineurin B-like protein; CPK = calcium-dependent protein kinase; SOS1 = Salt Overly Sensitively 1; AKT1 = *Arabidopsis thaliana* K^+ transporter; CNGC = cyclic-nucleotide gated channel; V-ATPase = vacuolar- ATPase; MAP = mitogen-activated protein; MAPK = mitogen-activated protein kinase; MAPKK = mitogen-activated protein kinase kinase; ROS = responsive oxygen species.

with that of previous studies that showed that ABA could reduce K^+ transport to the shoots and increase delivery of K^+ to the roots via the phloem to enhance the resistance of roots to water stress (Szczerba et al., 2009). Transgenic *ClAKT2* effectively relieves the slow growth of *A. thaliana* caused by potassium starvation, and transgenic plants can still grow normally under conditions of salt stress induced by potassium deficiency (–K+Na). We also found that the number of lateral roots of transgenic plants increased significantly compared with wild-type plants in the absence of K^+. It has been reported that *AtAKT2* is involved in energy conversion in the root, which can replace the sugar in the phloem and then circulate in the phloem under the action of ATP to disperse the energy storage function (Gajdanowicz et al*.,* 2011). It still needs further verification whether this finding is the theoretical basis for the increase in the number of lateral roots under potassium deficiency.

Conclusion

Our transcriptional profiling analysis revealed the genes and metabolic pathways that play critical roles in the reaction to salt stress in *C. lavandulifolium*. Species-specific reactions were observed when comparing the responsive genes' expression patterns between *C. lavandulifolium* and *C. ×morifolium*. We speculated that the species-specific mechanism governing salt tolerance in *C. lavandulifolium* could be the significantly greater induction of genes coding components of the ABA-dependent pathway, the SOS system, and multiple transporters, resulting in restricted uptake of toxic Na^+. In addition, the downstream responsive genes involved in flavonoid and proline biosynthesis may protect *C. lavandulifolium* cells from oxidative stress originating from salt and hence contribute to stress tolerance (Fig. 9). The results and resources produced in this investigation provide numerous salt-responsive genes for improving salt tolerance in *C. ×morifolium*. The results may also help direction transgenic breeding programs for *C. ×morifolium* to extend cultivation in high saline and drought soil environments.

Literature Cited

Andreasson, E. and B. Ellis. 2010. Convergence and specificity in the *Arabidopsis* MAPK nexus. Trends Plant Sci. 15:106–113.

Ardie, S.W., S.K. Liu, and T. Takano. 2010. Expression of the *AKT1*-type K^+ channel gene from *Puccinellia tenuiflora*, *PutAKT1*, enhances salt tolerance in *Arabidopsis*. Plant Cell Rpt. 29:865–874.

Audic, S. and J.M. Claverie. 1997. The significance of digital gene expression profiles. Genome Res. 7:986–995.

Aydi, S., S. Sassi, M. Debouba, K. Hessini, E. Larrainzar, H. Gouia, and C. Abdelly. 2010. Resistance of *Medicago truncatula* to salt stress is related to glutamine synthetase activity and sodium sequestration. J. Plant Nutr. Soil Sci. 173:892–899.

Bao, J., Y. Cai, M. Sun, G. Wang, and H. Corke. 2005. Anthocyanins, flavonols, and free radical scavenging activity of chinese bayberry (*Myrica rubra)* extracts and their color properties and stability. J. Agr. Food Chem. 53:2327–2332.

Bassil, E. and E. Blumwald. 2014. The ins and outs of intracellular ion homeostasis: NHX-type cation/H^+ transporters. Curr. Opin. Plant Biol. 22:1–6.

Bates, L., R. Waldren, and I. Teare. 1973. Rapid determination of free proline for water-stress studies. Plant Soil 39:205–207.

Baxter, A., R. Mittler, and N. Suzuki. 2014. ROS as key players in plant stress signalling. J. Expt. Bot. 65:1229–1240.

Bose, J., A. Rodrigo-Moreno, and S. Shabala. 2013. ROS homeostasis in halophytes in the context of salinity stress tolerance. J. Expt. Bot. 65:1241–1257.

Boyle, E.I., S. Weng, J. Gollub, H. Jin, D. Botstein, J.M. Cherry, and G. Sherlock. 2004. GO:TermFinder—Open source software for accessing gene ontology information and finding significantly enriched gene ontology terms associated with a list of genes. Bioinformatics 20:3710–3715.

Brunetti, C., M. Di Ferdinando, A. Fini, S. Pollastri, and M. Tattini. 2013. Flavonoids as antioxidants and developmental regulators: Relative significance in plants and humans. Intl. J. Mol. Sci. 14:3540–3555.
Chen, L., Y. Song, S. Li, L. Zhang, C. Zou, and D. Yu. 2012. The role of WRKY transcription factors in plant abiotic stresses. BBA-Gene Regulatory Mechanisms 1819:120–128.
Chen, Y.X., X.J. Zhou, S. Shu, Z.L. Chu, H.M. Wang, S.C. Han, and Y.D. Wang. 2017. Calcium-dependent protein kinase 21 phosphorylates 14-3-3 proteins in response to ABA signaling and salt stress in rice. Biochem. Biophys. Res. Commun. 493:1450–1456.
Clough, S.J. and A.F. Bent. 1998. Floral dip: A simplified method for *Agrobacterium*-mediated transformation of *Arabidopsis thaliana*. Plant J. 16:735–743.
Conesa, A., S. Götz, J.M. García-Gomez, J. Terol, M. Talon, and M. Robles. 2005. Blast2GO: A universal tool for annotation, visualization and analysis in functional genomics research. Bioinformatics 21:3674–3676.
Cristina, M.S., M. Petersen, and J. Mundy. 2010. Mitogen-activated protein kinase signaling in plants. Annu. Rev. Plant Biol. 61:621–649.
Dabbous, A., R. Ben Saad, F. Brini, A. Farthat-Khemekhem, W. Zorrig, C. Abdely, and K. Ben Hamed. 2017. Over-expression of a subunit E1 of a vacuolar H+-ATPase gene (Lm VHA-E1) cloned from the halophyte *Lobularia maritima* improves the tolerance of *Arabidopsis thaliana* to salt and osmotic stresses. Environ. Expt. Bot. 137:128–141.
Dang, Z.H., L.L. Zheng, J. Wang, Z. Gao, S.B. Wu, Z. Qi, and Y.C. Wang. 2013. Transcriptomic profiling of the salt-stress response in the wild recretohalophyte *Reaumuria trigyna*. BMC Genomics 14:29.
Deeken, R., D. Geiger, J. Fromm, O. Koroleva, P. Ache, R. Langenfeld-Heyser, N. Sauer, S.T. May, and R. Hedrich. 2002. Loss of the *AKT2/3* potassium channel affects sugar loading into the phloem of *Arabidopsis*. Planta 216:334–344.
Deinlein, U., A.B. Stephan, T. Horie, W. Luo, G. Xu, and J.I. Schroeder. 2014. Plant salt-tolerance mechanisms. Trends Plant Sci. 19:371–379.
Ding, Y., J. Cao, L. Ni, Y. Zhu, A. Zhang, M. Tan, and M. Jiang. 2013. *ZmCPK11* is involved in abscisic acid-induced antioxidant defence and functions upstream of *ZmMPK5* in abscisic acid signalling in maize. J. Expt. Bot. 64:871–884.
Dong, F.L., H. Huang, J. Liu, M. Zhang, Y.W. Zhou, and S.L. Dai. 2018. Cloning and function analysis of *ClNAC9* from *Chrysanthemum lavandulifolium*. Can. J. Plant Sci. 98:1265–1279.
Flowers, T.J. and T.D. Colmer. 2008. Salinity tolerance in halophytes. New Phytol. 179:945–963.
Flowers, T.J. and T.D. Colmer. 2015. Plant salt tolerance: Adaptations in halophytes. Ann. Bot. 115:327–331.
Gajdanowicz, P., E. Michard, M. Sandmann, M. Rocha, L.G. Corrêa, S.J. Ramírez-Aquilar, J.L. Gomez-Porras, W. González, J.B. Thibaud, J.T. van Dongen, and I. Dreyer. 2011. Potassium (K^+) gradients serve as a mobile energy source in plant vascular tissues. Proc. Natl. Acad. Sci. USA 108:864–869.
Gambale, F. and N. Uozumi. 2006. Properties of shaker-type potassium channels in higher plants. J. Membr. Biol. 210(1):1–19.
Gao, W.J., M. He, J. Liu, X. Ma, Y. Zhang, S.L. Dai, and Y.W. Zhou. 2018. Overexpression of *Chrysanthemum lavandulifolium ClCBF1* in *Chrysanthemum morifolium* 'White Snow' improves the level of salinity and drought tolerance. Plant Physiol. Biochem. 124:50–58.
Golldack, D., C. Li, H. Mohan, and N. Probst. 2014. Tolerance to drought and salt stress in plants: Unraveling the signaling networks. Front. Plant Sci. 5:151.
Grefen, C. and M.R. Blatt. 2012. Do calcineurin B-like proteins interact independently of the serine threonine kinase CIPK23 with the K^+ channel AKT1? Lessons learned from a menage a trois. Plant Physiol. 159:915–919.
Hasegawa, P.M. 2013. Sodium (Na^+) homeostasis and salt tolerance of plants. Environ. Expt. Bot. 92:19–31.
Heath, R.L. and L. Packer. 1968. Photoperoxidation in isolated chloroplasts: I. Kinetics and stoichiometry of fatty acid peroxidation. Arch. Biochem. Biophys. 125:189–198.
Huang, G.T., S.L. Ma, L.P. Bai, L. Zhang, H. Ma, P. Jia, J. Liu, M. Zhong, and Z.F. Guo. 2012. Signal transduction during cold, salt, and drought stresses in plants. Mol. Biol. Rpt. 39:969–987.
Huang, H., Y.J. Niu, H.W. Cao, X.J. Tang, X.L. Xia, W.L. Yin, and S.L. Dai. 2012a. cDNA-AFLP analysis of salt-inducible genes expression in *Chrysanthemum lavandulifolium* under salt treatment. J. Plant Physiol. 169:410–420.
Huang, H., Y. Wang, S. Wang, X. Wu, K. Yang, Y.J. Niu, and S.L. Dai. 2012b. Transcriptome-wide survey and expression analysis of stress-responsive *NAC* genes in *Chrysanthemum lavandulifolium*. Plant Sci. 193:18–27.
Jain, D. and D. Chattopadhyay. 2010. Analysis of gene expression in response to water deficit of chickpea (*Cicer arietinum* L.) varieties differing in drought tolerance. BMC Plant Biol. 10:24.
Jiang, Y. and M.K. Deyholos. 2006. Comprehensive transcriptional profiling of NaCl-stressed *Arabidopsis* roots reveals novel classes of responsive genes. BMC Plant Biol. 6:25.
Jiang, Y. and M.K. Deyholos. 2009. Functional characterization of *Arabidopsis* NaCl-inducible *WRKY25* and *WRKY33* transcription factors in abiotic stresses. Plant Mol. Biol. 69:91–105.
Katiyar-Agarwal, S., P. Verslues, and J. Zhu. 2005. Mechanisms of salt tolerance in plants. Plant Nutr. Food Security Human Health Environ. Protection 23:44–45.
Kim, B.G., R. Waadt, Y.H. Cheong, G.K. Pandey, J.R. Dominguez-Solis, S. Schültke, S.C. Lee, J. Kudla, and S. Luan. 2007. The calcium sensor CBL10 mediates salt tolerance by regulating ion homeostasis in *Arabidopsis*. Plant J. 52:473–484.
Kirsch, M., A. Zhigang, R. Viereck, R. Löw, and T. Rausch. 1996. Salt stress induces an increased expression of V-type H^+-ATPase in mature sugar beet leaves. Plant Mol. Biol. 32:543–547.
Lagarde, D., M. Basset, M. Lepetit, G. Conejero, F. Gaymard, S. Astruc, and C. Grignon. 1996. Tissue-specific expression of *Arabidopsis AKT1* gene is consistent with a role in K^+ nutrition. Plant J. 9:195–203.
Ling, R. and Z. Shi. 1983. Anthemideae. Flora Republicae Popularis Sinicae. Vol 76(1). Sci. Press, Beijing, China.
Liu, W.Z., M. Deng, L. Li, B. Yang, H. Li, H. Deng, and Y.Q. Jiang. 2015. Rapeseed calcineurin B-like protein CBL4, interacting with CBL-interacting protein kinase CIPK24, modulates salt tolerance in plants. Biochem. Biophys. Res. Commun. 467:467–471.
Natale, D.A., U.T. Shankavaram, M.Y. Galperin, Y.I. Wolf, L. Aravind, and E.V. Koonin. 2000. Towards understanding the first genome sequence of a crenarchaeon by genome annotation using clusters of orthologous groups of proteins (COGs). Genome Biol. 1(5):0009.1–0009.19.
Park, S.Y., P. Fung, N. Nishimura, D.R. Jensen, H. Fujii, Y. Zhao, S. Lumba, J. Santiago, A. Rodrigues, and F.C. Tsz-fung. 2009. Abscisic acid inhibits type 2C protein phosphatases via the PYR/PYL family of START proteins. Science 324:1068–1071.
Pasapula, V., G. Shen, S. Kuppu, J. Paez-Valencia, M. Mendoza, P. Hou, J. Chen, X. Qiu, L. Zhu, and X. Zhang. 2011. Expression of an *Arabidopsis* vacuolar H^{+-} pyrophosphatase gene (AVP1) in cotton improves drought- and salt tolerance and increases fibre yield in the field conditions. Plant Biotechnol. J. 9:88–99.
Pilot, G., F. Gaymard, K. Mouline, I. Chérel, and H. Sentenac. 2003a. Regulated expression of *Arabidopsis* shaker K^+ channel genes involved in K^+ uptake and distribution in the plant. Plant Mol. Biol. 51:773–787.
Pilot, G., R. Pratelli, F. Gaymard, Y. Meyer, and H. Sentenac. 2003b. Five-group distribution of the Shaker-like K^+ channel family in higher plants. J. Mol. Evol. 56:418–434.
Rady, M., W. Semida, T.A. Abd El-Mageed, K. Hemida, and M. Rady. 2018. Up-regulation of antioxidative defense systems by glycine

betaine foliar application in onion plants confer tolerance to salinity stress. Scientia Hort. 240:614–622.
Raghavendra, A.S., V.K. Gonugunta, A. Christmann, and E. Grill. 2010. ABA perception and signalling. Trends Plant Sci. 15:395–401.
Rivero, R.M., J.M. Ruiz, P.C. Garcıa, L.R. Lopez-Lefebre, E. Sánchez, and L. Romero. 2001. Resistance to cold and heat stress: Accumulation of phenolic compounds in tomato and watermelon plants. Plant Sci. 160:315–321.
Rozema, J. and H. Schat. 2013. Salt tolerance of halophytes, research questions reviewed in the perspective of saline agriculture. Environ. Expt. Bot. 92:83–95.
Sharma, S., J.G. Villamor, and P.E. Verslues. 2011. Essential role of tissue-specific proline synthesis and catabolism in growth and redox balance at low water potential. Plant Physiol. 157:292–304.
Silva, P. and H. Gerós. 2009. Regulation by salt of vacuolar H^+-ATPase and H^+-pyrophosphatase activities and Na^+/H^+ exchange. Plant Signal. Behav. 4:718–726.
Steinhorst, L. and J. Kudla. 2013. Calcium and reactive oxygen species rule the waves of signaling. Plant Physiol. 163:471–485.
Sutter, J.U., P. Campanoni, M. Tyrrell, and M.R. Blatt. 2006. Selective mobility and sensitivity to SNAREs is exhibited by the *Arabidopsis KAT1* K^+ channel at the plasma membrane. Plant Cell 18:935–954.
Suzuki, N., G. Miller, J. Morales, V. Shulaev, M.A. Torres, and R. Mittler. 2011. Respiratory burst oxidases: The engines of ROS signaling. Curr. Opin. Plant Biol. 14:691–699.
Szczerba, M.W., D.T. Britto, and H.J. Kronzucker. 2009. K^+ transport in plants: Physiology and molecular biology. J. Plant Physiol. 166:447–466.
Tamura, K., D. Peterson, N. Peterson, G. Stecher, M. Nei, and S. Kumar. 2011. MEGA5: Molecular evolutionary genetics analysis using maximum likelihood, evolutionary distance, and maximum parsimony methods. Mol. Biol. Evol. 28:2731–2739.
von Heijne, G. 1992. Membrane protein structure prediction. Hydrophobicity analysis and the positive-inside rule. J. Mol. Biol. 225:487–494.
Wang, J.C., B.C. Li, Y.C. Meng, X.L. Ma, Y. Lai, E. Si, Y. Yang, P.R. Ren, X.W. Shang, and H.J. Wang. 2015. Transcriptomic profiling of the salt-stress response in the halophyte *Halogeton glomeratus*. BMC Genomics 16:169.
Wang, J.C., B.C. Li, L.R. Yao, Y.X. Meng, X.L. Ma, Y. Lai, E.J. Si, P.R. Ren, K. Yang, X.W. Shang, and H.J. Wang. 2018a. Comparative transcriptome analysis of genes involved in Na^+ transport in the leaves of halophyte *Halogeton glomeratus*. Gene 678:407–416.
Wang, X.J., C. Guo, J. Peng, C. Li, F.F. Wan, S.M. Zhang, Y.Y. Zhou, Y. Yan, L.J. Qi, K.W. Sun, S.H. Yang, Z.Z. Gong, and J.G. Li. 2018b. ABRE-BINDING FACTORS play a role in the feedback regulation of ABA signaling by mediating rapid ABA induction of ABA co-receptor genes. New Phytol. (In press).
Wang, Y., H. Huang, Y.P. Ma, J.X. Fu, L.L. Wang, and S.L. Dai. 2014. Construction and de novo characterization of a transcriptome of *Chrysanthemum lavandulifolium*: Analysis of gene expression patterns in floral bud emergence. Plant Cell Tissue Organ Cult. 116:297–309.
Wei, S.W., L.W. Gao, Y.D. Zhang, F.R. Zhang, X. Yang, and D.F. Huang. 2016. Genome-wide investigation of the *NAC* transcription factor family in melon (*Cucumis melo* L.) and their expression analysis under salt stress. Plant Cell Rpt. 35:1827–1839.
Wixon, J. and D. Kell. 2000. The Kyoto Encyclopedia of Genes and Genomes—KEGG. Yeast 17:48–55.
Wu, Y.Q., W. Wei, X.Y. Pang, X.F. Wang, H.L. Zhang, B. Dong, Y.P. Xing, X.G. Li, and M.Y. Wang. 2014. Comparative transcriptome profiling of a desert evergreen shrub, *Ammopiptanthus mongolicus*, in response to drought and cold stresses. BMC Genomics 15:671.
Yokoi, S., F.J. Quintero, B. Cubero, M.T. Ruiz, R.A. Bressan, P.M. Hasegawa, and J.M. Pardo. 2002. Differential expression and function of *Arabidopsis thaliana* NHX Na^+/H^+ antiporters in the salt stress response. Plant J. 30:529–539.
Yoshida, T., J. Mogami, and K. Yamaguchi-Shinozaki. 2014. ABA-dependent and ABA-independent signaling in response to osmotic stress in plants. Curr. Opin. Plant Biol. 21:133–139.
Yu, Q.Y., L.J. An, and W.L. Li. 2014. The CBL-CIPK network mediates different signaling pathways in plants. Plant Cell Rpt. 33:203–214.
Yuan, Y., L.J. Qi, J. Yang, C. Wu, Y.J. Liu, and L.Q. Huang. 2015. A *Scutellaria baicalensis* R2R3-MYB gene, *SbMYB8*, regulates flavonoid biosynthesis and improves drought stress tolerance in transgenic tobacco. Plant Cell Tissue Organ Cult. 120:961–972.
Zarattini, M. and G. Forlani. 2017. Toward unveiling the mechanisms for transcriptional regulation of proline biosynthesis in the plant cell response to biotic and abiotic stress conditions. Front. Plant Sci. 8:927.
Zhang, L., D.M. Xi, S.W. Li, Z. Gao, S.L. Zhao, J. Shi, C.A. Wu, and X.Q. Guo. 2011. A cotton group C MAP kinase gene, *GhMPK2*, positively regulates salt and drought tolerance in tobacco. Plant Mol. Biol. 77:17–31.
Zhang, M., X. Wu, H. Huang, M. Zhou, and S.L. Dai. 2012. Salt tolerance analysis of four chrysanthemum (*Chrysanthemum* × *morifolium*) varieties. Adv. Ornamental Hort. China 2012:490–497.
Zhu, J.K. 2003. Regulation of ion homeostasis under salt stress. Curr. Opin. Plant Biol. 6:441–445.

Supplemental Table 1. Statistics of the upgraded version of the digital gene expression (DGE).

	CK[z]		S[y]	
Summary	CK no.	Proportion (%)	S no.	Proportion (%)
Total bps	591,654,224	100.00	573,971,006	100.00
Clean reads	12,074,576	0.99	11,713,694	99.15
Distinct unigene	84,944	100.00	89,217	100.00
Total mapped reads	4,086,043	33.84	4,013,617	34.26
Perfect match	3,036,658	25.15	3,022,338	25.80
≤2 bp mismatch	1,049,385	8.69	991,279	8.46
Unique match	4,082,685	33.81	4,009,663	34.23
Multiposition match	3,358	0.03	3,954	0.03
Total unmapped reads	7,988,533	66.16	7,700,077	65.74

[z]Control seedlings were treated with clear water for 12 h.
[y]Seedlings were treated with an equivalent amount of 200 mM sodium chloride for 12 h.

Supplemental Table 2. Numbers of differentially expressed genes (DEGs) related to hormone biosynthesis and signal transduction in *Chrysanthemum lavandulifolium* under salt treatment.

Family or pathway	DEGs (no.)	Up-regulated 2-fold (no.)	Down-regulated 2-fold (no.)	Up-regulated 5-fold (no.)	Down-regulated 5-fold (no.)
Hormone biosynthesis					
Ethylene biosynthesis	23	3	0	0	0
Jasmonic acid biosynthesis	2	0	0	0	0
Auxin	16	3	4	0	1
ABA	6	5	0	2	0
Cytokinin	13	3	2	2	0
Gibberellin	13	3	2	2	0
Signal transduction					
CaMs	5	4	0	0	0
CDPK	17	6	0	0	0
CBL-CIPK	17	8	0	4	0
MAPK	32	18	5	7	2
Wall-associated kinase	6	3	0	0	0
LRR	30	2	0	8	0
RLKs	18	4	1	1	0
PP2C	10	9	0	3	0
Serine/threonine phosphatases	27	3	0	0	0
Phospholipase D	13	5	1	0	1
PA	6	0	0	0	0

ABA = abscisic acid; CaMs = calmodulin genes; CDPK = calcium-dependent protein kinase; CBL-CIPK = calcineurin B-like protein-CBL-interacting protein kinase; MAPK = mitogen-activated protein kinase; LRR = leucine-rich repeat; RLKs = receptor-like kinases; PP2C = protein phosphatase 2C; PA = phosphatidic acid.

Supplemental Table 3. Numbers of differentially expressed genes (DEGs) encoding transcription factors in *Chrysanthemum lavandulifolium* under salt treatment.

TF family	DEGs (no.)	Up-regulated 2-fold (no.)	Down-regulated 2-fold (no.)	Up-regulated 5-fold (no.)	Down-regulated 5-fold (no.)
NAC	21	12	1	4	0
WRKY	22	13	0	4	0
AP2/EREBP	11	6	0	2	0
SBP	7	0	2	0	2
bHLH	10	1	1	0	0
HSF	8	1	0	1	0
TCP	9	3	1	0	0
bZIP	13	1	0	1	0
C2H2 zinc finger	6	0	1	0	0
ZF-HD	9	2	3	1	1
MYB	29	3	5	3	0
MADS	8	3	3	0	0
HB	11	2	1	1	0
JUMONJI	4	0	0	0	0
GRAS	8	1	0	1	0
C3H zinc finger	9	3	1	0	1

TF family = transcription factors family; NAC = NAM, ATAF1/2, CUC2; AP2/EREBP = apetala2/ethylene response element binding protein; SBP = squamosa promoter binding protein; bHLH = basic helix–loop–helix; HSF = heat shock factor; TCP = tb1, CYC, PCF1/2; bZIP = basic leucine zipper; C2H2 zinc finger = Cys2- His2 zinc finger; ZF-HD = zinc finger homeodomain; MYB = myeloblastosis; MADS = MCM-1, agamous, deficiens and serum response factor; HB = homeobox; GRAS = GAI, RGA, SCR; C3H zinc finger = Cys3- His zinc finger.

Supplemental Table 4. Numbers of differentially expressed genes (DEGs) related to transporters and phenylpropanoid biosynthesis pathways in *Chrysanthemum lavandulifolium* under salt treatment.

Family or pathway	DEGs (no.)	Up-regulated 2-fold (no.)	Down-regulated 2-fold (no.)	Up-regulated 5-fold (no.)	Down-regulated 5-fold (no.)
Transporters[z]					
Aquaporin	11	3	3	1	1
V-H^+- ATPase	16	8	1	4	1
PM-H^+- ATPase	10	4	0	1	0
V-H^+- PPase	5	3	0	1	0
Na^+/H^+ exchanger	10	7	1	4	1
HKT	3	2	0	2	0
AKT	5	2	1	0	0
CNGC	5	1	1	0	0
KUP	3	0	1	0	1
HAK	2	1	0	0	0
CHX	1	1	0	1	0
KOR	2	0	1	0	1
ClC	6	3	0	1	0
Sugar transporter	20	2	2	0	2
ABC transporter	22	9	6	3	0
Phenylpropanoid biosynthesis pathways	30	20	5	9	2

V-H+- ATPase = vacuolar H^+- ATPase; PM-H^+- ATPase = plasma membrane H^+- ATPase; V-H^+- PPase = vacuolar-type H^+-pumping pyrophosphatase; HKT = high-affinity K^+ transporter; AKT = *Arabidopsis thaliana* K^+ transporter; CNGC = cyclic-nucleotide gated channel; KUP = K^+ uptake premease; HAK = high affinity K^+; CHX = cation/H+ exchanger; KOR = potassium (K^+) outward rectifying channel; ClC = chloride channel; ABC transporter = ATP-binding cassette transporter.

Supplemental Table 5. Number of differentially expressed genes (DEGs) related to osmoprotection and responsive oxygen species (ROS)-scavenging system in *Chrysanthemum lavandulifolium* under salt treatment.

Family or pathway	DEGs (no.)	Up-regulated 2-fold (no.)	Down-regulated 2-fold (no.)	Up-regulated 5-fold (no.)	Down-regulated 5-fold (no.)
Osmoprotectants					
Proline	7	5	0	1	0
Trehalose biosynthesis	7	5	0	2	0
Dehydrin	8	0	1	0	0
		ROS-scavenging system			
RBOH	2	2	0	2	0
Dehydroascorbate reductase	5	3	1	0	0
Glutaredoxin	16	0	1	0	0
Ascorbate peroxidase	7	4	0	2	0
Glutathione peroxidase	5	1	0	0	0
Glutathione reductase	2	1	0	1	0
NADPH oxidase	2	1	0	0	0
Peroxiredoxin	4	3	0	0	0
Superoxide dismutase	10	7	0	2	1
Nudix hydrolase	7	4	0	1	0
Class III peroxidase	3	0	0	0	1
Glutathione-S-transferase	11	5	3	3	2

RBOH = respiratory burst oxidase homologue.